
Semi-Empirical Objective Functions for MCMC Proposal Optimization

Chris Cannella Vahid Tarokh

Department of ECE

Duke University

Durham, NC 27705

christopher.cannella@duke.edu

Abstract

We introduce and demonstrate a semi-empirical procedure for determining approximate objective functions suitable for optimizing arbitrarily parameterized proposal distributions in MCMC methods. Our proposed Ab Initio objective functions consist of the weighted combination of functions following constraints on their global optima and of coordinate invariance that we argue should be upheld by general measures of MCMC efficiency for use in proposal optimization. The coefficients of Ab Initio objective functions are determined so as to recover the optimal MCMC behavior prescribed by established theoretical analysis for chosen reference problems. Our experimental results demonstrate that Ab Initio objective functions maintain favorable performance and preferable optimization behavior compared to existing objective functions for MCMC optimization when optimizing highly expressive proposal distributions. We argue that Ab Initio objective functions are sufficiently robust to enable the confident optimization of MCMC proposal distributions parameterized by deep generative networks that extend beyond the traditional limitations of individual MCMC schemes.

1 Introduction

The development of efficient Markov Chain Monte Carlo (MCMC) proposal distributions is vital to enable numerical estimation and statistical inference in increasingly complicated problem domains. If we had an exact definition of the notion of MCMC efficiency, this could be accomplished by straightforward optimization over a set of proposal distributions. Past computational limitations encouraged the use of architecturally limited MCMC schemes that yield useful results for a wide range of target distributions, such as Random Walk Metropolis [1] (RWM), Metropolis Adjusted Langevin Diffusion [2] (MALA), and Hamiltonian Monte Carlo [3] (HMC). Although much research has been devoted to adaptive methods to improve MCMC performance, traditional adaptive methods [4, 5, 6, 7] focus on optimization across highly restricted proposal distribution model classes. Ideally, we would like to develop a practical method for optimizing MCMC performance over an arbitrarily parameterized class of proposal distributions.

Given their demonstrated success in parameterizing expressive distributions, deep generative models are naturally suited to the problem of MCMC proposal optimization. Despite the great freedom found within the model classes of generative models, current applications of deep learning to proposal optimization focus on the development of proposal architectures that either yield new restricted MCMC schemes [8, 9, 10] or extend existing schemes [11, 12, 13, 14]. A variety of objective functions are utilized to optimize these deep learning based approaches, with functional forms generally dependent on the type of MCMC scheme being optimized. We argue that the objective functions currently used for MCMC proposal optimization rely on the model class restrictions

imposed by selecting a particular MCMC scheme and may not be suitable for optimization across unrestricted proposal distributions easily implemented using current generative models. In this work, we introduce and demonstrate Ab Initio objective functions for MCMC proposal optimization intended to remain compatible with any proposal distribution defined using deep generative models.

Presumably, there exists some "ground truth" objective function underlying our notion of MCMC sampling performance. However, even after the decades of research regarding MCMC methods, there appears to be no universal definition for what we mean by MCMC efficiency. Metrics like effective sample size (ESS) [15, 16] generally coincide with our notion of sampling performance, but no such metric serves as the canonical definition of MCMC efficiency. Theoretical analysis regarding optimal acceptance rates for particular MCMC schemes [17, 18, 19, 20, 21] considers restricted proposal schemes and targets within a continuous diffusionary limit wherein our common performance metrics converge in their definition of optimality [17]. Within this diffusionary limit, useful properties regarding MCMC optimality (e.g. the rules of thumb to seek an acceptance rate of 0.234 when using RWM and of 0.574 when using MALA) may be derived without specifically defining sampling performance. In light of the lack of an exactly specified objective function for MCMC efficiency, our Ab Initio objective functions seek to approximate the ground truth definition of sampling performance by adhering to certain reasonable first principles properties and fitting to reproduce the "mathematical observations" provided by existing theoretical analysis of optimal acceptance rates.

Our contributions are as follows:

- We describe a set of first principles properties that may be reasonably assumed of the ground truth objective function underlying our notion of MCMC efficiency.
- We illustrate the construction of an example Ab Initio objective function via the combination of simpler objective functions with coefficients determined to reproduce analytically derived optimal behavior on a single reference problem.
- We verify the generality of the resulting Ab Initio objective function through its ability to closely reproduce analytically known optimal results for a wide range of optimization tasks beyond the reference problem used in its construction.
- We describe a normalizing flow based proposal distribution capable of approximating multiple disparate MCMC schemes, including independent resampling, RWM, and MALA.
- Through a series of illustrative experiments involving this multi-scheme proposal distribution, we demonstrate the advantages of Ab Initio objective functions for optimizing arbitrarily defined MCMC proposal distributions.

2 Relation to Prior Work

Ab Initio techniques [22, 23, 24] are used in the physical sciences to simulate systems that would otherwise be unobservable in a laboratory setting. These Ab Initio methods are founded on principled approximations of fundamental physical laws with parameters chosen to reproduce the physical properties of reference systems that can be observed. We take inspiration from these methods in the physical sciences in forming the methodology of this work.

The purpose of this work is to introduce a procedure for selecting objective functions for MCMC proposal optimization that are suited to the optimization of proposal model classes arbitrarily parameterized by deep generative models. Research into the applications of deep learning for MCMC proposal optimization [8, 9, 10, 11, 12, 13, 14] has yielded a number of potential candidates for this objective function. We therefore compare our Ab Initio objective functions to these candidates on the basis of their suitability for optimization of arbitrary proposal distributions.

Pure KL-divergence based objectives [11, 12, 25, 26] have found some success, particularly when optimizing resampling style schemes. These objectives are unable to properly optimize proposals within a diffusionary limit [27]. We therefore omit pure KL-divergence based objectives from the comparisons within this work.

Adversarial objectives have been used to optimize proposal distributions, notably with A-NICE-MC [8, 9]. We view adversarial training as a means of approximately optimizing an existing performance

measure (e.g. KL-divergence), rather than defining a fundamentally new performance measure. We therefore also omit adversarial objectives from the comparisons within this work.

Mean squared jump distance [28] (MSJD) remains a popular objective for optimizing proposals. Notably, L2HMC [13] is optimized using a modification of MSJD with a regularization intended to encourage mixing of the resulting Markov Chain. As shown in our experiments, both MSJD and L2HMC’s modification can produce arbitrarily non-ergodic Markov Chains when optimizing proposal distributions with position dependence. Our Ab Initio objective functions avoid this undesirable optimization behavior by maintaining i.i.d. resampling from the target as their unique global minima.

Recently, a Generalized Speed Measure (GSM) was proposed as an objective function for MCMC proposal optimization [27]. This objective function amounts to maximizing proposal entropy subject to the constraint of achieving a user specified acceptance rate. To attain optimal results using the GSM, a user must have significant prior knowledge regarding the interaction of their proposal model class with the target distribution to specify an optimal acceptance rate. As attaining fixed acceptance rates will require restricting the proposal model class, this requirement is likely detrimental to the optimization of very general neural architectures. A key advantage of our Ab Initio objective functions over the GSM is that they do not require prior knowledge to recover near optimal MCMC behavior (e.g. our Ab Initio objective function, whose construction only involved the knowledge of the optimal acceptance rate for RWM, recovers optimized MALA proposals with acceptance rates around 0.5).

Normalizing flows [29, 30, 31] are of particular interest for MCMC proposal optimization, as their ability to evaluate exact likelihoods enables, in principle, the direct optimization of objective functions relevant to MCMC performance. Our example multi-scheme proposal distribution is fundamentally similar to the scheme introduced in [10], which employs HMC within the latent space of a pre-fit normalizing flow to improve MCMC efficiency. Our proposal distribution differs from that in [10] by allowing both the flow’s transformation and the latent proposal distribution to be optimized to improve MCMC efficiency, rather than being fixed from the start.

3 MCMC Proposal Optimization

In this work, we consider the task of optimizing a proposal density $g_\theta(\vec{x}'|\vec{x})$ to sample from a target density $\pi(\vec{x})$ for a MCMC task. Proposals are accepted with rate $\alpha_{g_\theta, \pi}(\vec{x}'|\vec{x})$ that ensures the resulting Markov Chain converges towards $\pi(\vec{x})$. For this work, we restrict ourselves to Metropolis-Hastings type schemes, wherein $\alpha_{g_\theta, \pi}(\vec{x}'|\vec{x}) = \min\{1, \frac{\pi(\vec{x}')g_\theta(\vec{x}|\vec{x}')}{\pi(\vec{x})g_\theta(\vec{x}'|\vec{x})}\}$. For optimization, we utilize some measure of sampling performance to define an objective function $\mathcal{L}[g; \pi]$ that imposes an ordering over proposal distributions by defining $g_1 < g_2$ exactly when $\mathcal{L}[g_1; \pi] > \mathcal{L}[g_2; \pi]$. We do not seek to provide an argument for the application of deep learning methods to MCMC proposal optimization, so we will simply assume that all objective functions of interest are well-behaved for optimization via deep learning techniques (i.e. they are continuous and almost surely differentiable). We will also assume that all proposal and target densities considered are positive and non-singular.

Let G be the set of allowed proposals to consider during optimization and let \mathcal{D} be the group of almost sure diffeomorphisms over the space of our data. To perform optimization, we first select some $T \in \mathcal{D}$ that provides us with the coordinate system we will use for optimization. Defining:

$$T \circ f(\vec{z}) = f(T^{-1}(\vec{z})) \left| \frac{\partial T^{-1}(\vec{z})}{\partial \vec{z}} \right|$$

We finally optimize to find $g_{opt} = \operatorname{argmin}_{g \in G} \mathcal{L}[T \circ g; T \circ \pi]$.

4 Properties of the Ground Truth Objective Function \mathcal{L}^*

For us to sensibly pursue the task of MCMC proposal optimization, we must assume the existence of some ground truth objective, \mathcal{L}^* , that produces our notion of sampling performance. As previously stated, we currently do not know a universal definition for \mathcal{L}^* . We may, however, assume that the ground truth objective satisfies a number of first principles properties:

\mathcal{L}^* is Proper Define an objective function to be *proper* if it attains a unique global minimum at $g(\vec{x}'|\vec{x}) = \pi(\vec{x}')$ and $\alpha_{g, \pi}(\vec{x}'|\vec{x}) = 1$ for all \vec{x}', \vec{x} . The overall goal of our MCMC methodology is to

approximate perfect i.i.d. sampling from the target, π . We therefore find it uncontroversial to assume that \mathcal{L}^* is proper.

\mathcal{L}^* is Representation Independent Define an objective function, \mathcal{L} , to be *representation independent* over a group of almost sure diffeomorphisms \mathcal{T} if, for all $T \in \mathcal{T}$, and for all proposal distributions g_1, g_2 , $\mathcal{L}[g_1; \pi] > \mathcal{L}[g_2; \pi]$ if and only if $\mathcal{L}[T \circ g_1; T \circ \pi] > \mathcal{L}[T \circ g_2; T \circ \pi]$. Similarly, we will say \mathcal{L} is *representation invariant* over \mathcal{T} if $\mathcal{L}[T \circ g; T \circ \pi] = \mathcal{L}[g; \pi]$ for all g . If \mathcal{L}^* were not representation independent over \mathcal{D} , then our definition of sampling performance would depend on which $T \in \mathcal{D}/\mathcal{H}$ is used when computing the optimization, where \mathcal{H} is the maximal subgroup of \mathcal{D} over which \mathcal{L}^* remains representation independent. To fully justify an ordering, we would need to justify our selection of a particular member from \mathcal{D}/\mathcal{H} , which we should expect to be exceptionally burdensome. Of course, we usually have little prior justification for selecting a particular T and instead often use the coordinate system in which data was originally collected, perhaps applying some rescaling and recentering. Thus, unless contradicted by future experimental or theoretical results, we should assume that \mathcal{L}^* is at least representation independent.

\mathcal{L}^* Yields Established Optimal Results Prior theoretical analysis has established certain properties regarding optimal proposal distributions for a number of MCMC schemes under diffusionary limits. If \mathcal{L}^* is to correspond to the same notion of sampling performance, it must yield the same results. Thus, we should expect that optimization of \mathcal{L}^* will recover the properties established within these theoretical works when applied in the same diffusionary limits.

5 Constructing Ab Initio Objective Functions

Without knowing the exact form of \mathcal{L}^* , we must resort to finding a useful approximation. Although the assumptions of being proper and representation independent limit the functional class to which \mathcal{L}^* belongs, this functional class remains quite expansive. This situation is greatly simplified by restricting our consideration to representation invariant objective functions. As shown in Appendix A, the positive weighted combination of proper and representation invariant objective functions is itself a proper and representation invariant objective function.

This allows us to construct potential approximations of \mathcal{L}^* by the combination of simpler objective functions as weighted by hyperparameter coefficients. These hyperparameter coefficients can then be fit so as to recover optimal properties established within existing theoretical works. We call the resulting objective function an Ab Initio objective function.

For this work, we will consider a functional class of the form:

$$\mathcal{L}[g; \pi] = \mathbb{E}_{\vec{x} \sim \pi(\vec{x})} [D_{KL}(g(\vec{x}'|\vec{x}) || \pi(\vec{x}')) - A d \mathbb{E}_{\vec{x}' \sim g(\vec{x}'|\vec{x})} [\log \alpha(\vec{x}'|\vec{x})]] \quad (1)$$

Where A is a hyperparameter coefficient for fitting and d is the dimensionality of the target. This functional form is chosen for its ease of computation. The factor of d was chosen by some trial and error and yields favorable results for problems up to 10,000 dimensions. In Appendix B, we demonstrate that this functional class is proper and representation independent.

6 Fitting and Verifying Ab Initio Objective Functions

There are many possible approaches to fitting the coefficients of an Ab Initio objective function to recover optimal results over reference problems. Very general and principled methodologies for this fitting are provided by procedures like stochastic Levenberg-Marquardt optimization [32].

For simplicity, we determined A by manual trial and error to match the theoretical result that RWM has an optimal acceptance rate of 0.234 when targeting a multivariate gaussian of zero mean and identity covariance. As the theoretical results are set within the diffusionary limit of $d \rightarrow \infty$, we must match the theoretical result in a problem with sufficiently large dimension in practice. Here, we perform this match to theoretical reference on a problem with 1000 dimensions. We recovered the desired acceptance rate with $A = 0.18125$ and the Ab Initio objective function considered through the remainder of this work is therefore:

$$\mathcal{L}[g; \pi] = \mathbb{E}_{\vec{x} \sim \pi(\vec{x})} [D_{KL}(g(\vec{x}'|\vec{x}) || \pi(\vec{x}')) - 0.18125 d \mathbb{E}_{\vec{x}' \sim g(\vec{x}'|\vec{x})} [\log \alpha(\vec{x}'|\vec{x})]] \quad (2)$$

Table 1: Verification results from applying Ab Initio objective function of Equation (2) to multiple MCMC optimization tasks with analytically known optimal properties. Although fit to recover optimal behavior in one reference problem (shown in bold), the Ab Initio objective function retains good agreement with analytical results for a wide range of problems. Value means are reported to at most the first significant digit of standard error (reported in parentheses).

		$d = 100$		$d = 1000$		$d = 10000$		Analytic Exact
		Ab Initio Eq. (2)	Analytic Simulated	Ab Initio Eq. (2)	Analytic Simulated	Ab Initio Eq. (2)	Analytic Simulated	
Reference Problem								
Gaussian	RWM	Acc. Rate	0.246(2)	0.236(1)	0.233(5)	0.234(1)	0.228(6)	0.235(2)
		MSJD	1.32(2)	1.32(1)	1.32(1)	1.324(4)	1.33(1)	1.33(1)
Scheme Robustness								
Gaussian	MALA	Acc. Rate	0.546(5)	0.572(2)	0.503(5)	0.572(2)	0.495(9)	0.573(3)
		MSJD	38.6(2)	38.4(2)	166(1)	167(1)	738(6)	748(3)
Target Robustness								
Uniform	RWM	Acc. Rate	0.146(9)	0.135(2)	0.146(1)	0.134(2)	0.144(9)	0.137(2)
		MSJD	8.2(1)e-3	8.2(1)e-3	8.5(1)e-4	8.4(1)e-4	8.5(2)e-5	8.6(1)e-5
Laplace	RWM	Acc. Rate	0.231(4)	0.234(3)	0.226(4)	0.234(2)	0.229(2)	0.235(2)
		MSJD	1.47(2)	1.48(2)	1.37(1)	1.37(1)	1.33(2)	1.34(1)
Cauchy	RWM	Acc. Rate	0.237(3)	0.235(2)	0.236(5)	0.234(1)	0.233(3)	0.233(2)
		MSJD	2.72(3)	2.72(3)	2.67(3)	2.64(1)	2.67(3)	2.61(2)
Dimensional Robustness								

By fitting the parameters of an Ab Initio objective function, we hope to approximate a general notion of MCMC efficiency beyond the particularities of the reference problem(s) used in its construction. To verify this robustness, we utilized the Ab Initio function listed in Equation (2) to perform MCMC optimization in a number of tasks where the optimal acceptance rate is analytically known, with varying target distribution (independent gaussian, laplace, cauchy, and uniform), dimensionality (100-10,000 dimensions), and MCMC scheme (RWM with gaussian proposals and MALA). These tasks are all within the diffusional limit and involve a severely limited model class for proposal distributions (optimizing only proposal step size). Under these limitations, acceptance rate adequately summarizes differences between optimized model parameters and MSJD adequately summarizes the efficiency of the resulting Markov Chains. These measures are estimated for each optimized model based on 25,000 proposals from starting points independently sampled from the target distribution. To gather statistics regarding the mean and standard error of reported variables, each verification optimization is replicated a total 5 times. These results are listed in Table 1. Additional experimental details and results are provided in Appendix C.

We find that the Ab Initio objective of Equation (2) exhibits good agreement with known analytical results beyond the reference problem used in its construction. The best agreement, both in acceptance rate and resulting MSJD, is obtained in the RWM optimization tasks with continuous target densities. Even though the objective was tuned to replicate optimal behavior when optimizing RWM for a 1000 dimensional Gaussian target, the Ab Initio objective is also able to reproduce optimal behavior when optimizing a MALA proposal against a continuous target (recovering an acceptance rate around 0.5) and when optimizing RWM proposal against a discontinuous target (recovering an acceptance rate around 0.145). With one exception (the 10000 dimensional MALA optimization experiment, where the difference in MSJD is less than 2%), the difference in MSJD performance between the Ab Initio and analytically optimized proposals is statistically insignificant.

These results demonstrate that the Ab Initio objective remains a useful approximation of our notion of MCMC efficiency across a wide range of optimization problems within the diffusional limit for which we have analytically known solutions. At the same time, defining the Ab Initio objective to be proper ensures, in principle, valid optimization behaviour in the opposite asymptotic limit of model complexity wherein i.i.d. resampling from the target lies within the proposal distribution's model class. While the Ab Initio objective does not perfectly match our definition of MCMC efficiency,

these results indicate that the Ab Initio objective is a sufficiently robust approximation to be used with confidence in MCMC proposal optimization tasks with arbitrary proposal and target distributions.

7 Experimental Results

To demonstrate the advantages of Ab Initio objective functions, we present a series of illustrative experiments. In these experiments, we compare objective functions on the basis of their capabilities for optimizing very general parameterizations of proposal distributions that should be of interest for MCMC proposal optimization. We emphasize that the purpose of these experiments is not to advocate for any particular proposal architecture or scheme. Throughout these experiments, we use effective sample size (ESS) as a measure of sampling performance. We consider one-dimensional ESS relating to uncertainty estimating first and second moments of the target distribution's marginals, reporting the minimum obtained across all dimensions. For comparisons, we consider MSJD optimization [28] (MSJD Opt.), L2HMC's objective [13] (L2HMC Obj.), and the Generalized Speed Measure [27] targeting acceptance rates of 0.9, 0.6, and 0.3 (GSM-90, -60, and -30). Additional experimental details and results are provided in Appendices E, F, and G.

7.1 Optimizing Position Dependent Mixture Proposals

To examine general objective function behavior without additional complications arising from particular proposal architectures, we first consider the optimization of proposals consisting of a mixture of gaussians (with position independent means and covariances) with position dependent component weights specified by a neural network. This proposal distribution may be specified as follows:

$$\begin{aligned} \vec{x}' | \vec{x}, (S = i) &\sim \mathcal{N}\{\mu_{i,\theta}; \Sigma_{i,\theta}\} \\ P(S = i | \vec{x}) &= f_\theta(\vec{x}) \end{aligned} \tag{3}$$

For this experiment, we target a 2 dimensional target that is an equal mixture of 4 gaussians positioned in a cross formation. Our proposal class consists of 4 gaussian components with position dependent weights and is therefore capable of i.i.d. resampling of the target. Because we are primarily interested in the properties of the global optima of the compared objective functions in this task, rather than the engineering details of attaining those optima in this specific task, we initialize the proposals to start near i.i.d. resampling. For each optimization, we determine efficiency measures on the basis of 5 Markov Chains of 1000 total proposals starting from independent samples from the target distribution. Statistics regarding the mean and standard error of these measures are collected from 5 replications for each considered objective function. The results of these optimizations are provided in Table 2.

Density plots of the position dependent weighting functions obtained following optimization using an MSJD objective and our Ab Initio objective are provided in Figure 1. We find that i.i.d. resampling remains a stable global minimum of our Ab Initio objective function. The GSM objective also optimizes towards a constant and equal weighting of the proposals components, but increases the variance of each component to match its targeted acceptance rate. Both MSJD and L2HMC's modification find global minima at arbitrarily non-ergodic proposals. Both of these MSJD based objectives result in Markov Chains that only effectively explore half of the target's probability mass (either the horizontal or vertical components), which is numerically reflected by the poor ESS performance for estimating second moments.

7.2 Optimizing Multi-Scheme Proposals

We now introduce a normalizing flow based proposal distribution. With T_θ denoting a normalizing flow's parameterized transformation, the functions $\mu_{L,\theta}$, $\mu_{D,\theta}$, $\Sigma_{L,\theta}$, and $\Sigma_{D,\theta}$ specified by neural networks, and \odot denoting element wise multiplication, our proposal distribution is defined via:

$$\begin{aligned} \vec{n} &\sim \mathcal{N}\{\vec{0}; I\} \\ \vec{z}' | \vec{x}, \vec{n} &= \mu_{L,\theta}(T_\theta^{-1}(\vec{x})) + \Sigma_{L,\theta}(T_\theta^{-1}(\vec{x})) \odot \vec{n} \\ \vec{x}' &= \mu_{D,\theta}(\vec{x}) + \Sigma_{D,\theta}(\vec{x}) \odot T_\theta(\vec{z}') \end{aligned} \tag{4}$$

This implementation is fundamentally a conditional normalizing flow [33]. In Appendix D, we demonstrate how this parameterization is able to approximate or recover various existing MCMC

Table 2: Comparison of sampling performance obtained optimizing the position-dependent mixture proposals of Equation (3) using various objective functions. Value means are reported to at most the first significant digit of standard error (reported in parentheses).

	Acc. Rate	MSJD	ESS per Proposal	
			x_i	x_i^2
Ab Initio, Eq. (2)	0.998(1)	34.0(3)	1.00(2)	1.05(3)
MSJD Opt. [28]	0.998(1)	65.9(4)	1.00(1)	6(1)e-4
L2HMC Obj. [13]	0.998(1)	66.0(2)	1.01(1)	7(1)e-4
GSM-90 [27]	0.900(2)	30.8(3)	0.81(2)	0.81(6)
GSM-60 [27]	0.601(5)	20.9(2)	0.41(2)	0.40(4)
GSM-30 [27]	0.297(7)	10.3(4)	0.15(1)	0.16(1)
I.I.D. Resample	1.000	34.2(2)	0.96(5)	1.01(3)

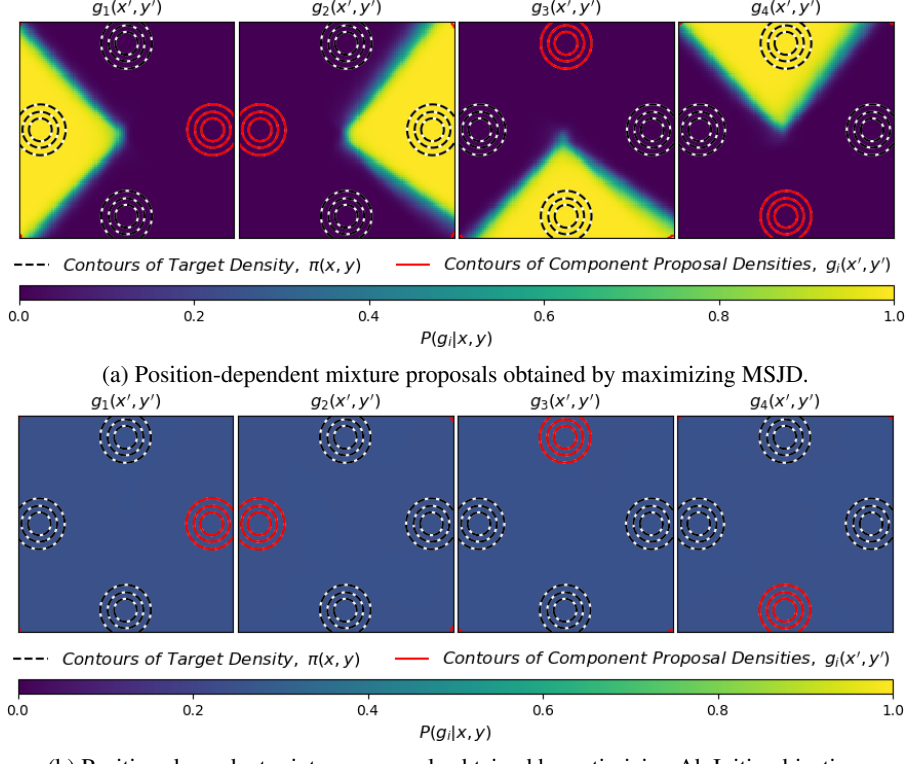


Figure 1: Comparison of position-dependent mixture proposals of Equation (3) obtained by maximizing MSJD (a) and optimizing Ab Initio objective (b). Each subplot illustrates the contours of a proposal component (in red) alongside a density plot of the probability of sampling from that component based on starting position.

schemes. Optimization of this proposal distribution encompasses both selection of MCMC scheme (e.g. whether RWM or approximate resampling is more efficient) and selection of optimal parameters within a given scheme (e.g. RWM step size). Depending on the network architectures used for this proposal’s implementation, it may be more or less adept at approximating particular schemes for a given target distribution. We therefore have little a priori knowledge of this proposal distribution’s optimal acceptance rates for arbitrary target distributions, presenting fundamental difficulties for optimization of the GSM objective. The flexibility of this parameterization is also obtained using position dependent networks, which can lead to undesirable behaviour when optimizing using MSJD based objectives. For this experiment, we use the mixture of gaussians target from the previous section. We use the NICE architecture [34] to define the normalizing flow and vary the number of coupling layers (using either 8 or 3 layers), which influences how accurately the flow is able to approximate the target distribution. For each optimization, we determine efficiency measures on the basis of 5 Markov Chains of 1000 total proposals starting from independent samples from the target

Table 3: Comparison of sampling performance obtained optimizing the multi-scheme proposals of Equation (4) using various objective functions. Results are reported for two choices for the number of coupling layers used in the proposal’s normalizing flow ($L = 8$ and $L = 3$). Value means are reported to at most the first significant digit of standard error (reported in parentheses).

	L=8				L=3			
	Acc. Rate	MSJD	ESS per Proposal		Acc. Rate	MSJD	ESS per Proposal	
			x_i	x_i^2			x_i	x_i^2
Ab Initio, Eq. (2)	0.67(3)	22(1)	0.33(5)	0.41(5)	0.55(4)	17(1)	0.18(8)	0.2(1)
MSJD Opt. [28]	0.975(6)	66.2(9)	1.10(3)	6(1)e-4	0.978(4)	67(1)	1.10(3)	7(1)e-4
L2HMC Obj. [13]	0.974(3)	65.7(5)	1.12(2)	6(1)e-4	0.974(5)	66(1)	1.11(1)	6.1(3)e-4
GSM-90 [27]	0.92(1)	1.86(5)	5.6(4)e-4	7(1)e-4	0.90(2)	1.80(4)	5.3(4)e-4	7(1)e-4
GSM-60 [27]	0.65(6)	21(2)	0.3(2)	0.3(2)	0.60(1)	1.41(1)	6(1)e-4	1(1)e-3
GSM-30 [27]	0.31(1)	10.7(4)	0.14(2)	0.17(1)	0.302(6)	10.5(4)	0.13(2)	0.18(2)
I.I.D. Resample	1.00	34.4(3)	0.98(5)	0.99(6)	1.00	33.9(3)	0.90(7)	1.03(5)

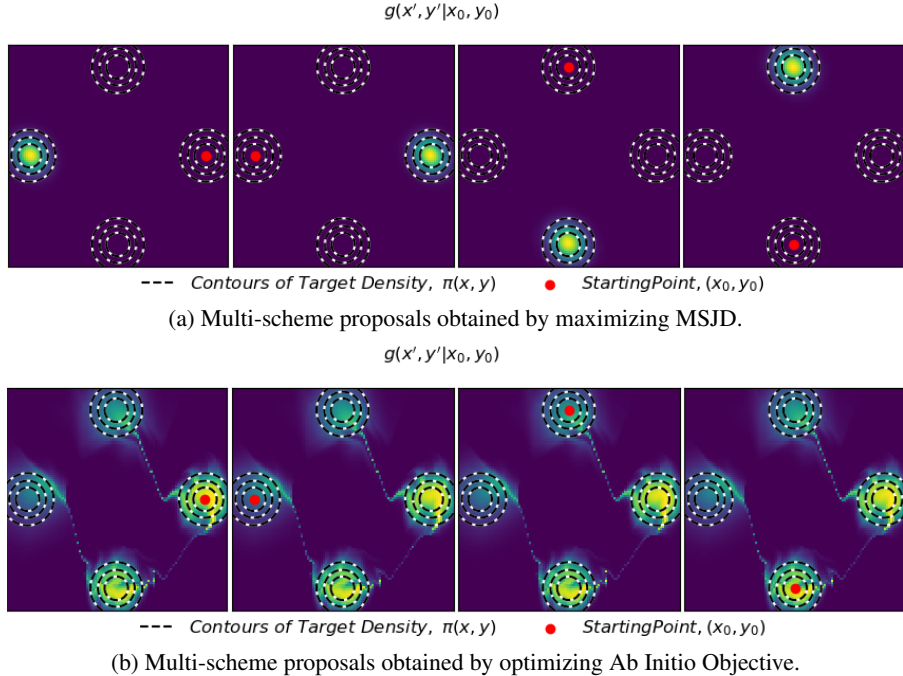


Figure 2: Comparison of multi-scheme mixture proposals ($L=8$) of Equation (4) obtained by maximizing MSJD (a) and optimizing Ab Initio objective (b). Each subplot illustrates the proposal distribution’s density when sampling from a given starting position (in red).

distribution. Statistics regarding the mean and standard error of these measures are collected from 5 replications for each considered objective function. The results of these optimizations are provided in Table 3.

Density plots of multi-scheme proposal distributions obtained following optimization using an MSJD objective and our Ab Initio objective are provided in Figure 2. The Ab Initio objective is able to optimize towards efficient approximations of independent resampling. As before, position dependence within the proposal distribution lead MSJD and L2HMC’s modification to optimize towards arbitrarily non-ergodic proposal distributions.

This experiment demonstrates an additional problem in applying the GSM objective to arbitrary proposal distributions. For this flow based proposal, the flow’s depth determines it’s maximal accuracy in approximating independent resampling of the target distribution, creating a maximum acceptance rate that can be obtained while still approximating global resampling. For this proposal distribution, attaining greater acceptance rates is possible, but forces inefficient RWM-like behavior. In this case,

Table 4: Comparison of sampling performance obtained optimizing augmented multi-scheme proposals of Equation (4) using various objective functions targeting posterior distributions of parameters for logistic regression of UCI datasets. Value means are reported to at most the first significant digit of standard error (reported in parentheses).

	German Credit (d=21)				Heart Disease (d=14)			
	Acc. Rate	MSJD	ESS per Proposal		Acc. Rate	MSJD	ESS per Proposal	
			x_i	x_i^2			x_i	x_i^2
Ab Initio, Eq. (2)	0.81(1)	0.30(1)	0.56(3)	0.49(7)	0.86(2)	1.03(4)	0.63(6)	0.58(7)
MSJD Opt. [28]	0.77(2)	0.32(1)	0.52(7)	0.4(1)	0.81(1)	1.40(3)	0.69(3)	0.32(6)
L2HMC Obj. [13]	0.76(2)	0.32(1)	0.54(4)	0.48(5)	0.82(1)	1.43(4)	0.73(4)	0.28(7)
GSM-90 [27]	0.90(1)	0.012(1)	0.006(1)	0.005(1)	0.900(3)	0.138(3)	0.034(2)	0.035(1)
GSM-60 [27]	0.61(3)	0.24(1)	0.40(3)	0.40(3)	0.59(2)	0.72(2)	0.34(3)	0.35(3)
GSM-30 [27]	0.29(5)	0.13(2)	0.13(4)	0.13(4)	0.29(3)	0.42(4)	0.13(2)	0.14(3)
HMC	0.65	0.201(3)	0.006(3)	0.005(3)	0.65	0.70(1)	0.02(1)	0.02(1)

8 coupling layers within the flow permits a maximal resampling acceptance rate near 0.70, which means GSM optimization targeting a rate of 0.90 yields inefficient RWM-like proposals. Using 3 coupling layers lowers this maximal rate below 0.60, which means GSM optimization targeting a rates of both 0.60 and 0.90 yield inefficient RWM-like proposals. In general, the value of this acceptance rate threshold will not be known a priori, and could be arbitrarily low. No acceptance rate can be safely assumed to yield efficient behavior without restricting the proposal’s model class.

7.3 Optimizing Augmented Multi-Scheme Proposals for Bayesian Logistic Regression

To demonstrate the application of Ab Initio objectives to MCMC optimization tasks of a more practical nature, we consider the optimization of the multi-scheme proposals defined in Equation (4) for MCMC sampling of regression weights in bayesian logistic regression for various UCI datasets [35]. As augmentation with auxiliary variables (e.g. the momenta of HMC) are a common feature of MCMC schemes [13, 12], we augment the original distributions with a number of independent auxiliary variables equal to the distribution’s original dimensionality. For each optimization, we determine efficiency measures on the basis of 5 Markov Chains of 20000 total proposals starting from samples drawn from a long, equilibrated Markov Chain obtained using tuned HMC. Statistics regarding the mean and standard error of these measures are collected from 5 replications for each considered objective function. The results of these optimizations are provided in Table 4.

8 Conclusion and Future Work

In this work, we have shown how to construct Ab Initio objective functions that are suited for the optimization of arbitrary proposal distributions. Our experimental results show that Ab Initio objective functions can maintain favorable performance and preferable optimization behavior compared to existing objective functions [13, 27, 28] when optimizing proposal distributions of a relatively unrestricted model class. By design, Ab Initio objective functions are approximations of our notion of MCMC efficiency and we do not presume that the particular example Ab Initio objective function of Equation (2) will be absolutely universal. There may be proposal architectures and target distributions for which the objective function in Equation (2) yields sub-optimal results. However, our proposed Ab Initio procedure allows for further improvements by considering alternative component functions and coefficient fitting procedures, which we plan to explore in future work.

The experimental methodology this work is intended to isolate fundamental effects of the choice of objective function on MCMC optimization. How to best train proposals distributions in an online adaptive setting, how to attain computationally efficient samples, and how to handle scaling into higher dimensions remain important practical considerations for MCMC optimization. We argue that these considerations are primarily influenced by proposal architecture and training procedure selection. We will therefore investigate these questions in a future work focusing on comparisons among specific proposal architectures and training procedures.

We find that Ab Initio objectives are suitably robust to enable the optimization of highly expressive MCMC proposal distributions. In this work, we’ve used a normalizing flow based multi-scheme

proposal distribution as a prototypical example. As future work, we plan to research improved multi-scheme proposal architectures that better leverage the potential of deep generative models for MCMC optimization.

Acknowledgements and Disclosure of Funding

This work was supported by the Office of Naval Research (ONR) under grant number N00014-18-1-2244.

References

- [1] Nicholas Metropolis, Arianna W Rosenbluth, Marshall N Rosenbluth, Augusta H Teller, and Edward Teller. Equation of State Calculations by Fast Computing Machines. *The Journal of Chemical Physics*, 21(6):1087–1092, 1953.
- [2] Julian Besag and Peter J Green. Spatial Statistics and Bayesian Computation. *Journal of the Royal Statistical Society: Series B (Methodological)*, 55(1):25–37, 1993.
- [3] Simon Duane, Anthony D Kennedy, Brian J Pendleton, and Duncan Roweth. Hybrid Monte Carlo. *Physics Letters B*, 195(2):216–222, 1987.
- [4] Gareth O Roberts and Jeffrey S Rosenthal. Examples of Adaptive MCMC. *Journal of Computational and Graphical Statistics*, 18(2):349–367, 2009.
- [5] Dino Sejdinovic, Heiko Strathmann, Maria Lomeli Garcia, Christophe Andrieu, and Arthur Gretton. Kernel Adaptive Metropolis-Hastings. In *International Conference on Machine Learning*, pages 1665–1673. PMLR, 2014.
- [6] Heikki Haario, Eero Saksman, Johanna Tamminen, et al. An Adaptive Metropolis Algorithm. *Bernoulli*, 7(2):223–242, 2001.
- [7] Gareth O Roberts and Jeffrey S Rosenthal. Coupling and Ergodicity of Adaptive Markov Chain Monte Carlo Algorithms. *Journal of Applied Probability*, 44(2):458–475, 2007.
- [8] Jiaming Song, Shengjia Zhao, and Stefano Ermon. A-NICE-MC: Adversarial Training for MCMC. In *Proceedings of the 31st International Conference on Neural Information Processing Systems*, pages 5146–5156, 2017.
- [9] Span Spanbauer, Cameron Freer, and Vikash Mansinghka. Deep Involutive Generative Models for Neural MCMC. *arXiv preprint arXiv:2006.15167*, 2020.
- [10] Matthew Hoffman, Pavel Sountsov, Joshua V Dillon, Ian Langmore, Dustin Tran, and Srinivas Vasudevan. Neutra-lizing Bad Geometry in Hamiltonian Monte Carlo Using Neural Transport. *arXiv preprint arXiv:1903.03704*, 2019.
- [11] Nando de Freitas, Pedro Højen-Sørensen, Michael I Jordan, and Stuart Russell. Variational MCMC. In *Proceedings of the Seventeenth Conference on Uncertainty in Artificial Intelligence*, pages 120–127, 2001.
- [12] Raza Habib and David Barber. Auxiliary Variational MCMC. In *International Conference on Learning Representations*, 2018.
- [13] Daniel Levy, Matthew D Hoffman, and Jascha Sohl-Dickstein. Generalizing Hamiltonian Monte Carlo with Neural Networks. *International Conference on Learning Representations*, 2018.
- [14] Zengyi Li, Yubei Chen, and Friedrich T Sommer. A Neural Network MCMC Sampler that Maximizes Proposal Entropy. *Entropy*, 23(3):269, 2021.
- [15] Andrew Gelman, John B Carlin, Hal S Stern, David B Dunson, Aki Vehtari, and Donald B Rubin. *Bayesian Data Analysis*. CRC press, 2013.
- [16] Dootika Vats, James M Flegal, and Galin L Jones. Multivariate Output Analysis for Markov Chain Monte Carlo. *Biometrika*, 106(2):321–337, 2019.
- [17] Gareth O Roberts, Jeffrey S Rosenthal, et al. Optimal Scaling for Various Metropolis-Hastings Algorithms. *Statistical Science*, 16(4):351–367, 2001.
- [18] Andrew Gelman, Walter R Gilks, and Gareth O Roberts. Weak Convergence and Optimal Scaling of Random Walk Metropolis Algorithms. *The Annals of Applied Probability*, 7(1):110–120, 1997.

[19] Gareth O Roberts and Jeffrey S Rosenthal. Optimal Scaling of Discrete Approximations to Langevin Diffusions. *Journal of the Royal Statistical Society: Series B (Statistical Methodology)*, 60(1):255–268, 1998.

[20] Peter Neal, Gareth Roberts, Wai Kong Yuen, et al. Optimal Scaling of Random Walk Metropolis Algorithms with Discontinuous Target Densities. *Annals of Applied Probability*, 22(5):1880–1927, 2012.

[21] Alexandros Beskos, Natesh Pillai, Gareth Roberts, Jesus-Maria Sanz-Serna, Andrew Stuart, et al. Optimal Tuning of the Hybrid Monte Carlo Algorithm. *Bernoulli*, 19(5A):1501–1534, 2013.

[22] Warren J Hehre. Ab Initio Molecular Orbital Theory. *Accounts of Chemical Research*, 9(11):399–406, 1976.

[23] MT Yin and Marvin L Cohen. Theory of Ab Initio Pseudopotential Calculations. *Physical Review B*, 25(12):7403, 1982.

[24] Dominik Marx and Jürg Hutter. *Ab Initio Molecular Dynamics: Basic Theory and Advanced Methods*. Cambridge University Press, 2009.

[25] Kirill Neklyudov, Evgenii Egorov, Pavel Shvchikov, and Dmitry Vetrov. Metropolis-Hastings View on Variational Inference and Adversarial Training. *arXiv preprint arXiv:1810.07151*, 2018.

[26] Tongzhou Wang, Yi Wu, David A Moore, and Stuart J Russell. Meta-Learning MCMC Proposals. *Proceedings of the 32nd International Conference on Neural Information Processing Systems*, 2018.

[27] Michalis Titsias and Petros Dellaportas. Gradient-Based Adaptive Markov Chain Monte Carlo. *Advances in Neural Information Processing Systems*, 32:15730–15739, 2019.

[28] Cristian Pasarica and Andrew Gelman. Adaptively Scaling the Metropolis Algorithm Using Expected Squared Jumped Distance. *Statistica Sinica*, pages 343–364, 2010.

[29] Esteban G Tabak and Cristina V Turner. A Family of Nonparametric Density Estimation Algorithms. *Communications on Pure and Applied Mathematics*, 66(2):145–164, 2013.

[30] Danilo Rezende and Shakir Mohamed. Variational Inference with Normalizing Flows. In *International Conference on Machine Learning*, pages 1530–1538. PMLR, 2015.

[31] George Papamakarios, Eric Nalisnick, Danilo Jimenez Rezende, Shakir Mohamed, and Balaji Lakshminarayanan. Normalizing Flows for Probabilistic Modeling and Inference. *arXiv preprint arXiv:1912.02762*, 2019.

[32] E Bergou, Y Diouane, V Kungurtsev, and CW Royer. A Stochastic Levenberg-Marquardt Method Using Random Models with Application to Data Assimilation. *arXiv preprint arXiv:1807.02176*, 2018.

[33] Christina Winkler, Daniel Worrall, Emiel Hoogeboom, and Max Welling. Learning Likelihoods with Conditional Normalizing Flows. *arXiv preprint arXiv:1912.00042*, 2019.

[34] Laurent Dinh, David Krueger, and Yoshua Bengio. Nice: Non-linear Independent Components Estimation. *arXiv preprint arXiv:1410.8516*, 2014.

[35] Kevin Bache and Moshe Lichman. UCI Machine Learning Repository, 2013.

[36] Diederik P Kingma and Jimmy Ba. Adam: A Method for Stochastic Optimization. In *ICLR (Poster)*, 2015.

[37] Anand Patil, David Huard, and Christopher J Fonnesbeck. PyMC: Bayesian Stochastic Modelling in Python. *Journal of Statistical Software*, 35(4):1, 2010.

[38] Brian D Ripley. *Pattern Recognition and Neural Networks*. Cambridge University Press, 2007.

[39] Adam D Cobb, Atilim Güneş Baydin, Andrew Markham, and Stephen J Roberts. Introducing an Explicit Symplectic Integration Scheme for Riemannian Manifold Hamiltonian Monte Carlo. *arXiv preprint arXiv:1910.06243*, 2019.

A Combining Proper and Representation Invariant Functions

As part of our Ab Initio approach, we rely on the following proposition:

Proposition: Every positive weighted combination of proper and representation invariant objective functions is itself a proper and representation invariant objective function.

To prove this, assume that we have two proper and representation invariant (over a group of almost sure diffeomorphisms \mathcal{D}) objective functions f and h with target π and allowed set of proposals \mathcal{G} . Let us select arbitrary constants $c_1, c_2 > 0$ and consider the properties of the objective function $c_1f + c_2h$. From the invariance of f and h we may immediately conclude:

$$\begin{aligned}(c_1f + c_2h)[T \circ g; T \circ \pi] &= c_1f[T \circ g; T \circ \pi] + c_2h[T \circ g; T \circ \pi] \\ &= c_1f[g; \pi] + c_2h[g; \pi] \\ &= (c_1f + c_2h)[g; \pi]\end{aligned}$$

Hence $c_1f + c_2h$ is itself representation invariant. Finally, for all $g(x'|x) \neq \pi(x')$:

$$\begin{aligned}(c_1f + c_2h)[\pi; \pi] &= c_1f[\pi; \pi] + c_2h[\pi; \pi] \\ &< c_1f[g; \pi] + c_2h[g; \pi] = (c_1f + c_2h)[g; \pi]\end{aligned}$$

Hence $c_1f + c_2h$ is also proper. This concludes the proof of the above proposition.

This offers a straightforward approach to approximating our ground truth objective \mathcal{L}^* . Although we do not have a guarantee that \mathcal{L}^* lies within the class of representation invariant objective functions (we have only assumed representation independence), we also have too few analytical results to empirically conclude that \mathcal{L}^* is not representation invariant. As fitting the coefficients of an Ab Initio objective function to match analytical results is more easily accomplished than deriving a particular objective function that happens to match analytical results, we argue that our Ab Initio approach is a practical method for obtaining approximate objective functions suitable for the optimization of arbitrary MCMC proposal distributions.

Next, we slightly extend this result in order to justify the functions composing Equation 1 of the main paper. Below, we start with a definition.

Definition: An objective function is said to be *nearly proper* if it attains a (not necessarily unique) global minimum at $g(\vec{x}'|\vec{x}) = \pi(\vec{x}')$ and $\alpha_{g,\pi}(\vec{x}'|\vec{x}) = 1$ for all \vec{x}', \vec{x} .

We may now consider a minor generalization of the previous proposition:

Proposition: Every positive weighted combination of at least one proper and representation invariant objective function with any number of nearly proper and representation independent functions is itself a proper and representation invariant objective function.

The proof that the resulting combination is representation invariant follows from the representation invariance of the component functions, exactly as in the above. To show that the combination is proper, assume that we have representation invariant (over a group of almost sure diffeomorphisms \mathcal{D}) objective functions f and h with target π and allowed set of proposals \mathcal{G} . Let f be proper and let h be nearly proper. Let us select arbitrary constants $c_1, c_2 > 0$ and consider the properties of the objective function $c_1f + c_2h$. For all $g(x'|x) \neq \pi(x')$:

$$\begin{aligned}(c_1f + c_2h)[\pi; \pi] &= c_1f[\pi; \pi] + c_2h[\pi; \pi] \\ &\leq c_1f[\pi; \pi] + c_2h[g; \pi] \\ &< c_1f[g; \pi] + c_2h[g; \pi] = (c_1f + c_2h)[g; \pi]\end{aligned}$$

Hence $c_1f + c_2h$ is also proper.

B Properties of Our Example Ab Initio Objective Function

The functional form of our example Ab Initio objective function is given by:

$$\mathcal{L}[g; \pi] = \mathbb{E}_{\vec{x} \sim \pi(\vec{x})} [D_{KL}(g(\vec{x}'|\vec{x}) || \pi(\vec{x}')) - C(d) \mathbb{E}_{\vec{x}' \sim g(\vec{x}'|\vec{x})} [\log \alpha(\vec{x}'|\vec{x})]]$$

Where $C(d)$ is a dimension dependent positive constant. We will now consider the following proposition:

Proposition: The example Ab Initio objective function, $\mathcal{L}[g; \pi]$, defined above is a proper and representation independent objective function for all $C(d) \geq 0$.

Following the general restrictions we've used to define our optimization problem, let g and π be positive and smooth and let T denote any almost sure diffeomorphism. Let \mathcal{X}_T and \mathcal{Z}_T denote the regions of the domain and range of T over which T is differentiable and invertible. From the properties of KL-Divergence, we know that $\mathbb{E}_{\vec{x} \sim \pi(\vec{x})} [D_{KL}(g(\vec{x}'|\vec{x}) || \pi(\vec{x}'))] \geq 0$ and is equal to 0 if and only if $g(\vec{x}'|\vec{x}) = \pi(\vec{x}')$ for all \vec{x}, \vec{x}' . From the definition of KL-Divergence and the law of the unconscious statistician, we have:

$$\begin{aligned} \mathbb{E}_{\vec{x} \sim \pi(\vec{x})} [D_{KL}(g(\vec{x}'|\vec{x}) || \pi(\vec{x}'))] &= \mathbb{E}_{\vec{x} \sim \pi(\vec{x})} \left[\int_{\mathcal{X}_T} g(\vec{x}'|\vec{x}) \log \frac{g(\vec{x}'|\vec{x})}{\pi(\vec{x}')} d\vec{x}' \right] \\ &= \mathbb{E}_{\vec{z} \sim T \circ \pi(\vec{z})} \left[\int_{\mathcal{X}_T} g(\vec{x}'|\vec{z}) \log \frac{g(\vec{x}'|\vec{z})}{\pi(\vec{x}')} d\vec{x}' \right] \\ &= \mathbb{E}_{\vec{z} \sim T \circ \pi(\vec{z})} \left[\int_{\mathcal{Z}_T} T \circ g(\vec{z}'|\vec{z}) \log \frac{T \circ g(\vec{z}'|\vec{z})}{T \circ \pi(\vec{z}')} d\vec{z}' \right] \\ &= \mathbb{E}_{\vec{x} \sim T \circ \pi(\vec{x})} [D_{KL}(T \circ g(\vec{x}'|\vec{x}) || T \circ \pi(\vec{x}'))] \end{aligned}$$

Hence, $\mathbb{E}_{\vec{x} \sim \pi(\vec{x})} [D_{KL}(g(\vec{x}'|\vec{x}) || \pi(\vec{x}'))]$ is a proper and representation invariant objective function.

Next, for all proposals g and targets π , the Metropolis-Hastings acceptance rate is guaranteed to fall in the range $0 \leq \alpha(\vec{x}'|\vec{x}) \leq 1$. Additionally, if $g(\vec{x}'|\vec{x}) = \pi(\vec{x}')$, $\alpha(\vec{x}'|\vec{x}) = 1$. This guarantees that $\mathbb{E}_{\vec{x} \sim \pi(\vec{x})} [\mathbb{E}_{\vec{x}' \sim g(\vec{x}'|\vec{x})} [-\log \alpha(\vec{x}'|\vec{x})]]$ is nearly proper. And from the definition of the Metropolis-Hastings acceptance rate and the law of the unconscious statistician, we have:

$$\begin{aligned} \mathbb{E}_{\vec{x} \sim \pi(\vec{x})} [\mathbb{E}_{\vec{x}' \sim g(\vec{x}'|\vec{x})} [-\log \alpha(\vec{x}'|\vec{x})]] &= \mathbb{E}_{\vec{x} \sim \pi(\vec{x})} [\mathbb{E}_{\vec{x}' \sim g(\vec{x}'|\vec{x})} [-\log \alpha(\vec{x}'|\vec{x})]] \\ &= \mathbb{E}_{\vec{x} \sim \pi(\vec{x})} [\mathbb{E}_{\vec{x}' \sim g(\vec{x}'|\vec{x})} [-\log \min\{1, \frac{\pi(\vec{x}')g(\vec{x}|\vec{x}')}{\pi(\vec{x})g(\vec{x}'|\vec{x})}\}]] \\ &= \mathbb{E}_{\vec{z} \sim T \circ \pi(\vec{z})} [\mathbb{E}_{\vec{z}' \sim T \circ g(\vec{z}'|\vec{z})} [-\log \min\{1, \frac{\pi(T^{-1}(\vec{z}'))g(T^{-1}(\vec{z})|\vec{z}')}{\pi(T^{-1}(\vec{z}))g(T^{-1}(\vec{z}')|\vec{z})}\}]] \\ &= \mathbb{E}_{\vec{z} \sim T \circ \pi(\vec{z})} [\mathbb{E}_{\vec{z}' \sim T \circ g(\vec{z}'|\vec{z})} [-\log \min\{1, \frac{T \circ \pi(\vec{z}')T \circ g(\vec{z}|\vec{z}')}{T \circ \pi(\vec{z})T \circ g(\vec{z}'|\vec{z})}\}]] \\ &= \mathbb{E}_{\vec{x} \sim T \circ \pi(\vec{x})} [\mathbb{E}_{\vec{x}' \sim T \circ g(\vec{x}'|\vec{x})} [-\log \alpha(\vec{x}'|\vec{x})]] \end{aligned}$$

And so $\mathbb{E}_{\vec{x} \sim \pi(\vec{x})} [\mathbb{E}_{\vec{x}' \sim g(\vec{x}'|\vec{x})} [-\log \alpha(\vec{x}'|\vec{x})]]$ is a nearly proper and coordinate invariant objective function. With $C(d) \geq 0$, our example Ab Initio objective function is therefore the positive weighted combination of a proper and representation invariant objective function with a nearly proper and representation invariant function. From the previous section, we know that this example Ab Initio objective function is itself proper and representation invariant. As representation invariance implies representation independence, this example objective function is also representation independent and thus belongs to the same functional class as our approximated "ground truth" objective.

C Additional Data for Verification Tasks

For verification tests, we optimize objective functions for MCMC proposals targeting isotropic gaussian, laplace, cauchy, and uniform distributions with dimensionalities between 100 and 10,000. For numerical stability, our target uniform distribution is a mixture distribution of a standard uniform distribution and a standard multivariate gaussian (with probabilities of $\frac{1}{1+e^{-100}}$ and $\frac{1}{1+e^{100}}$ respectively, to provide some non-zero likelihood beyond the support of the uniform distribution). For optimization, 20000 gradient steps are taken, with each training batch taken from a single starting point sampled i.i.d. from the target distribution from which 50 proposals are generated to calculate expected loss. Optimization is performed using the Adam optimizer [36] with a stepsize of 3e-4 (reduced to 3e-5, 3e-6, and 3e-7 for uniform targets of dimensions 100, 1000, and 10000). For optimizing GSM [27], β is initially set to d^{-1} and ρ_β is set to 0.02. Acceptance rate and MSJD are estimated for each optimized model based on 25000 proposals from starting points independently sampled from the target distribution. To gather statistics regarding the mean and standard error of reported variables, each verification optimization is replicated a total 5 times. Tables 5, 6, 7, 8, and 9 report results from optimizing all objective functions we use in the main work for comparison with our example Ab Initio objective function. In these tables, simulated analytic results are also reported, which refer to acceptance rate and MSJD as estimated in the same manner for proposals with a fixed step size determined to yield the analytically known optimal acceptance rates.

We were unable to perform gradient based optimization of MSJD and L2HMC’s objective when targeting the uniform distribution, and resorted to estimating their optima by fitting curves of these objective functions with respect to acceptance rate. For MSJD, the results reported for MSJD targeting uniform distributions are therefore the result of fitting a parabola near the objective function’s maxima, with uncertainties reported following the typical propagation of error. Even following this procedure, L2HMC’s objective function is unable to produce non-trivial optima when targeting the uniform distribution and we therefore consider RWM optimization targeting the uniform distribution a failure case for L2HMC’s objective.

Table 5: Verification results from applying MSJD maximization to the MCMC optimization tasks with analytically known optimal properties. As these verification tasks are set within the diffusional limit, MSJD recovers known optimal results. Value means are reported to at most the first significant digit of standard error (reported in parentheses).

			$d = 100$		$d = 1000$		$d = 10000$		Analytic Exact
			MSJD Opt.	Analytic Simulated	MSJD Opt.	Analytic Simulated	MSJD Opt.	Analytic Simulated	
Gaussian	RWM	Acc. Rate	0.237(4)	0.235(1)	0.232(3)	0.234(3)	0.233(2)	0.234(2)	0.234 [17, 18]
		MSJD	1.32(2)	1.32(1)	1.32(1)	1.32(3)	1.33(2)	1.33(2)	
Gaussian	MALA	Acc. Rate	0.538(6)	0.574(1)	0.559(5)	0.573(1)	0.56(1)	0.574(2)	0.574 [17, 19]
		MSJD	38.6(1)	38.4(1)	167(1)	166(1)	749(2)	747(5)	
Uniform	RWM	Acc. Rate	0.15(2)	0.135(5)	0.15(2)	0.137(4)	0.134(2)	0.132(3)	0.135 [17, 20]
		MSJD	8.2(7)e-3	8.2(3)e-3	8.4(5)e-4	8.6(2)e-4	8.4(4)e-5	8.2(2)e-5	
Laplace	RWM	Acc. Rate	0.21(2)	0.234(1)	0.23(1)	0.233(1)	0.24(1)	0.234(3)	0.234 [17, 18]
		MSJD	1.48(1)	1.48(1)	1.37(2)	1.37(0)	1.34(1)	1.34(2)	
Cauchy	RWM	Acc. Rate	0.223(5)	0.235(3)	0.230(8)	0.235(3)	0.23(2)	0.235(2)	0.234 [17, 18]
		MSJD	2.72(3)	2.74(5)	2.65(1)	2.67(3)	2.64(2)	2.65(1)	

Table 6: Verification results from applying L2HMC’s objective to the MCMC optimization tasks with analytically known optimal properties. L2HMC’s objective only recovers optimal behavior for MALA proposals and cannot be used to optimize RWM proposals with a uniform target. Value means are reported to at most the first significant digit of standard error (reported in parentheses).

		$d = 100$		$d = 1000$		$d = 10000$		Analytic Exact	
		L2HMC Obj.	Analytic Simulated	L2HMC Obj.	Analytic Simulated	L2HMC Obj.	Analytic Simulated		
Gaussian	RWM	Acc. Rate	0.587(3)	0.233(3)	0.580(4)	0.235(1)	0.56(1)	0.233(1)	0.234 [17, 18]
		MSJD	0.69(1)	1.31(1)	0.71(1)	1.34(1)	0.76(4)	1.32(1)	
Gaussian	MALA	Acc. Rate	0.546(5)	0.575(2)	0.553(6)	0.575(3)	0.562(6)	0.574(1)	0.574 [17, 19]
		MSJD	38.6(2)	38.5(2)	167(1)	167(1)	750(3)	749(2)	
Uniform	RWM	Acc. Rate	—	—	—	—	—	—	0.135 [17, 20]
		MSJD	—	—	—	—	—	—	
Laplace	RWM	Acc. Rate	0.57(1)	0.235(2)	0.59(1)	0.233(2)	0.59(1)	0.234(2)	0.234 [17, 18]
		MSJD	0.78(4)	1.48(1)	0.71(3)	1.37(1)	0.69(2)	1.34(1)	
Cauchy	RWM	Acc. Rate	0.514(4)	0.235(2)	0.516(5)	0.237(1)	0.52(1)	0.236(1)	0.234 [17, 18]
		MSJD	1.77(3)	2.71(2)	1.77(3)	2.69(1)	1.74(5)	2.66(4)	

Table 7: Verification results from applying GSM targeting acceptance rates of 0.3 to the MCMC optimization tasks with analytically known optimal properties. Optimal behavior is approximately recovered only for RWM proposals at this acceptance rate. Value means are reported to at most the first significant digit of standard error (reported in parentheses).

		$d = 100$		$d = 1000$		$d = 10000$		Analytic Exact	
		GSM-30	Analytic Simulated	GSM-30	Analytic Simulated	GSM-30	Analytic Simulated		
Gaussian	RWM	Acc. Rate	0.298(4)	0.235(2)	0.295(4)	0.234(2)	0.299(9)	0.234(2)	0.234 [17, 18]
		MSJD	1.28(1)	1.33(2)	1.29(1)	1.32(1)	1.30(1)	1.33(1)	
Gaussian	MALA	Acc. Rate	0.297(6)	0.575(1)	0.295(8)	0.575(2)	0.297(6)	0.573(3)	0.574 [17, 19]
		MSJD	31.8(5)	38.4(3)	134(2)	167(1)	595(7)	748(3)	
Uniform	RWM	Acc. Rate	0.302(6)	0.135(1)	0.30(1)	0.136(2)	0.30(1)	0.135(2)	0.135 [17, 20]
		MSJD	6.6(2)e-3	8.18(7)e-3	6.8(2)e-4	8.6(2)e-4	6.9(1)e-5	8.4(1)e-5	
Laplace	RWM	Acc. Rate	0.303(6)	0.234(3)	0.29(1)	0.235(3)	0.32(1)	0.236(1)	0.234 [17, 18]
		MSJD	1.43(1)	1.48(1)	1.34(2)	1.38(2)	1.29(2)	1.34(1)	
Cauchy	RWM	Acc. Rate	0.297(2)	0.234(3)	0.291(3)	0.237(1)	0.30(1)	0.234(2)	0.234 [17, 18]
		MSJD	2.62(3)	2.71(4)	2.58(3)	2.69(1)	2.57(3)	2.65(2)	

Table 8: Verification results from applying GSM targeting acceptance rates of 0.6 to the MCMC optimization tasks with analytically known optimal properties. Optimal behavior is approximately recovered only for MALA proposals at this acceptance rate. Value means are reported to at most the first significant digit of standard error (reported in parentheses).

			$d = 100$		$d = 1000$		$d = 10000$		Analytic Exact
			GSM-60	Analytic Simulated	GSM-60	Analytic Simulated	GSM-60	Analytic Simulated	
Gaussian	RWM	Acc. Rate	0.602(2)	0.234(1)	0.60(1)	0.234(2)	0.60(1)	0.233(2)	0.234 [17, 18]
		MSJD	0.66(0)	1.31(1)	0.66(2)	1.33(1)	0.65(2)	1.32(1)	
Gaussian	MALA	Acc. Rate	0.607(7)	0.575(1)	0.60(1)	0.575(1)	0.596(5)	0.576(2)	0.574 [17, 19]
		MSJD	38.1(2)	38.5(2)	166(0)	167(0)	743(4)	751(4)	
Uniform	RWM	Acc. Rate	0.61(1)	0.135(2)	0.58(1)	0.135(1)	0.57(4)	0.138(1)	0.135 [17, 20]
		MSJD	2.4(1)e-3	8.20(9)e-3	2.7(1)e-4	8.52(8)e-4	2.8(4)e-5	8.64(4)e-5	
Laplace	RWM	Acc. Rate	0.60(1)	0.234(2)	0.61(3)	0.233(2)	0.63(4)	0.237(1)	0.234 [17, 18]
		MSJD	0.69(3)	1.48(1)	0.64(6)	1.37(2)	0.6(1)	1.35(1)	
Cauchy	RWM	Acc. Rate	0.599(6)	0.235(2)	0.603(5)	0.236(3)	0.60(1)	0.234(2)	0.234 [17, 18]
		MSJD	1.33(3)	2.72(2)	1.31(3)	2.69(3)	1.31(4)	2.64(3)	

Table 9: Verification results from applying GSM targeting acceptance rates of 0.9 to the MCMC optimization tasks with analytically known optimal properties. Results are significantly suboptimal. Value means are reported to at most the first significant digit of standard error (reported in parentheses).

			$d = 100$		$d = 1000$		$d = 10000$		Analytic Exact
			GSM-90	Analytic Simulated	GSM-90	Analytic Simulated	GSM-90	Analytic Simulated	
Gaussian	RWM	Acc. Rate	0.900(3)	0.234(2)	0.900(2)	0.232(2)	0.910(6)	0.233(2)	0.234 [17, 18]
		MSJD	0.06(0)	1.31(1)	0.06(2)	1.32(1)	0.05(1)	1.32(1)	
Gaussian	MALA	Acc. Rate	0.899(2)	0.575(1)	0.901(2)	0.576(2)	0.902(2)	0.574(1)	0.574 [17, 19]
		MSJD	20.6(3)	38.5(1)	92(1)	167(1)	421(4)	750(2)	
Uniform	RWM	Acc. Rate	0.90(1)	0.136(2)	0.90(2)	0.133(3)	0.95(5)	0.135(2)	0.135 [17, 20]
		MSJD	1.5(3)e-4	8.2(1)e-3	1.8(7)e-5	8.4(2)e-4	1(1)e-6	8.5(1)e-5	
Laplace	RWM	Acc. Rate	0.905(5)	0.234(2)	0.91(1)	0.235(2)	0.90(2)	0.234(1)	0.234 [17, 18]
		MSJD	0.05(1)	1.47(1)	0.05(1)	1.38(2)	0.06(2)	1.38(2)	
Cauchy	RWM	Acc. Rate	0.901(4)	0.234(1)	0.901(2)	0.235(2)	0.898(5)	0.233(2)	0.234 [17, 18]
		MSJD	0.11(1)	2.73(1)	0.11(0)	2.65(2)	0.12(1)	2.65(3)	

D Approximating MCMC Schemes with Multi-Scheme Proposals

As part of our experiments, we utilize a normalizing flow based multi-scheme proposal distribution, parameterized as:

$$\begin{aligned}\vec{n} &\sim \mathcal{N}\{\vec{0}; I\} \\ \vec{z}'|\vec{x}, \vec{n} &= \mu_{L,\theta}(T_\theta^{-1}(\vec{x})) + \Sigma_{L,\theta}(T_\theta^{-1}(\vec{x})) \odot \vec{n} \\ \vec{x}' &= \mu_{D,\theta}(\vec{x}) + \Sigma_{D,\theta}(\vec{x}) \odot T_\theta(\vec{z}')\end{aligned}$$

Where T_θ denotes a normalizing flow's parameterized transformation, the functions $\mu_{L,\theta}$, $\mu_{D,\theta}$, $\Sigma_{L,\theta}$, and $\Sigma_{D,\theta}$ are specified by neural networks, and \odot denotes element wise multiplication. This section provides examples of how this multi-scheme distribution is able to approximate many different existing MCMC schemes. Throughout, let π denote the target distribution, g_θ denote the density of the resulting proposal distribution, and let n denote the density of a standard gaussian distribution with zero mean and identity covariance.

Independent Resampling: If $T_\theta \circ n \approx \pi$, $\mu_{L,\theta} = \mu_{D,\theta} = \vec{0}$, and $\Sigma_{L,\theta} = \Sigma_{D,\theta} = \vec{1}$, then:

$$g_\theta(\vec{x}'|\vec{x}) \approx \pi(\vec{x}')$$

Depending on the accuracy of the flow's approximation, the multi-scheme distribution approximately recovers i.i.d. resampling from the target.

Isotropic RWM: If $T_\theta = I$, $\mu_{L,\theta} = \vec{0}$, $\mu_{D,\theta}(\vec{x}) = \vec{x}$, $\Sigma_{L,\theta} = \vec{1}$, and $\Sigma_{D,\theta} = \tau$, then:

$$\vec{x}'|\vec{x} \sim \mathcal{N}\{\vec{x}; \tau I\}$$

And the multi-scheme distribution recovers isotropic RWM with step-size τ .

Isotropic MALA: If $T_\theta = I$, $\mu_{L,\theta} = \vec{0}$, $\mu_{D,\theta}(\vec{x}) \approx \vec{x} + \tau \nabla \log \pi(\vec{x})$, $\Sigma_{L,\theta} = \vec{1}$, and $\Sigma_{D,\theta} = \sqrt{2\tau}$, then:

$$\vec{x}'|\vec{x} \sim \mathcal{N}\{\vec{x} + \tau \nabla \log \pi(\vec{x}); \sqrt{2\tau} I\}$$

Depending on the accuracy of the approximation of $\mu_{D,\theta}(\vec{x})$, the multi-scheme distribution recovers isotropic MALA with step-size τ .

Preconditioned Diffusions: If $T_\theta(\vec{z}) \approx A^{-1}\vec{z}$, where A is an invertible preconditioning matrix, then appropriate choices of $\mu_{L,\theta}$, $\mu_{D,\theta}$, $\Sigma_{D,\theta}$, and $\Sigma_{L,\theta}$ will approximately recover preconditioned RWM and MALA.

Latent MALA: If $T_\theta \circ n \approx \pi$, $\mu_{L,\theta}(\vec{x}) \approx (1 + \tau) \vec{x}$, $\mu_{D,\theta} = \vec{0}$, $\Sigma_{L,\theta} = \sqrt{2\tau}$, and $\Sigma_{D,\theta} = \vec{1}$, then the multi-scheme distribution will mimic the normalizing flow based proposal scheme of Hoffman et al. [10], with MALA used within the flow's latent space rather than HMC.

These examples are not exhaustive. Depending on implementation, these flow-based multi-scheme distributions could also parameterize useful proposal distributions that are not covered by existing MCMC schemes. An appealing aspect multi-scheme distributions is that their optimization, in theory, solves the problem of selecting which MCMC scheme to apply to a particular problem, which otherwise usually requires some intervention from the user. However, their expressiveness means that we cannot rely on guarantees that would be provided by restricting to individual MCMC schemes.

E Further Details for Position-Dependent Mixture Proposal Optimization

Our experiments with position-dependent mixture proposals utilize a distribution specified as follows:

$$\begin{aligned}\vec{x}'|\vec{x}, (S = i) &\sim \mathcal{N}\{\mu_{i,\theta}; \Sigma_{i,\theta}\} \\ P(S = i|\vec{x}) &= f_\theta(\vec{x})\end{aligned}$$

The target distribution is an equal mixture of 4 standard gaussians positioned in a cross formation with a maximal distance of 8 between component centers. The proposal distribution consists of 4 gaussian components. The position-dependent weights, $f_\theta(\vec{x})$, are specified by a standard ReLU

network (input dimension 2, hidden dimension 16, 4 hidden layers, output dimension 4) followed by a component-wise softmax layer. Proposals are initialized near i.i.d. sampling of the target. For optimization, 40000 gradient steps are taken, with each training batch taken from a single starting point sampled i.i.d. from the target distribution from which 50 proposals are generated to calculate expected loss. Optimization is performed using the Adam optimizer [36] with a stepsize of 3e-4. For optimizing GSM [27], β is initially set to 0.5 and ρ_β is set to 0.002. Acceptance rate, MSJD, and ESS are estimated for each optimized model based on 5 independent Markov Chains of 1000 proposals with starting points independently sampled from the target distribution. ESS relating to the second moments of the target distribution is estimated based on the Markov Chains obtained by component-wise squaring of the Markov Chains used to estimate the other performance measures. We utilize PyMC's [37] calculation of ESS, which considers both within-chain and between-chain variance. To gather statistics regarding the mean and standard error of reported variables, each optimization is replicated a total 5 times. Figures 3, 4, 5, and 6 show density plots of the position-dependent weighting functions obtained following optimization using L2HMC's objective [13] and the GSM [27] with varying target acceptance rates.

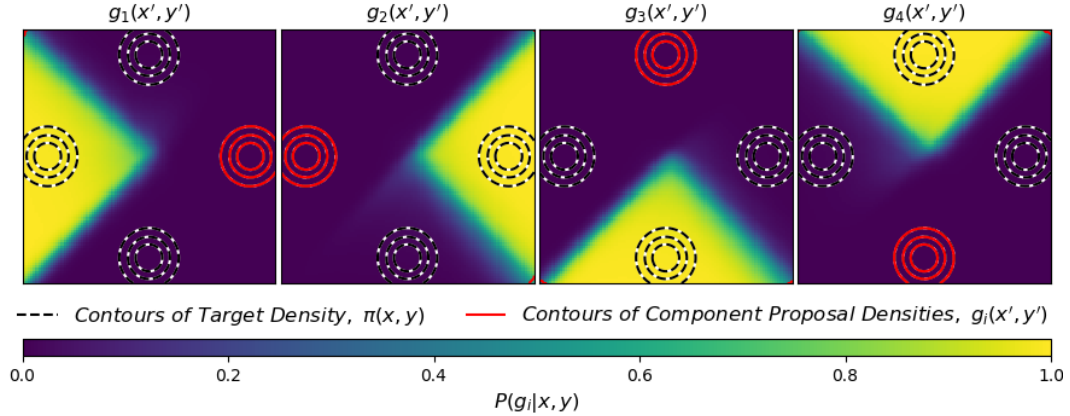


Figure 3: Comparison of position-dependent mixture proposals of Equation 3 obtained by optimizing L2HMC's objective. Each subplot illustrates the contours of a proposal component (in red) alongside a density plot of the probability of sampling from that component based on starting position.

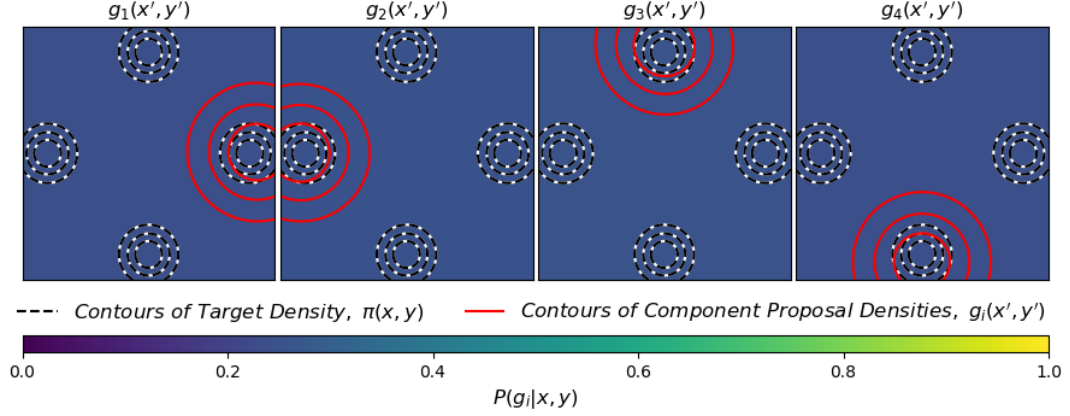
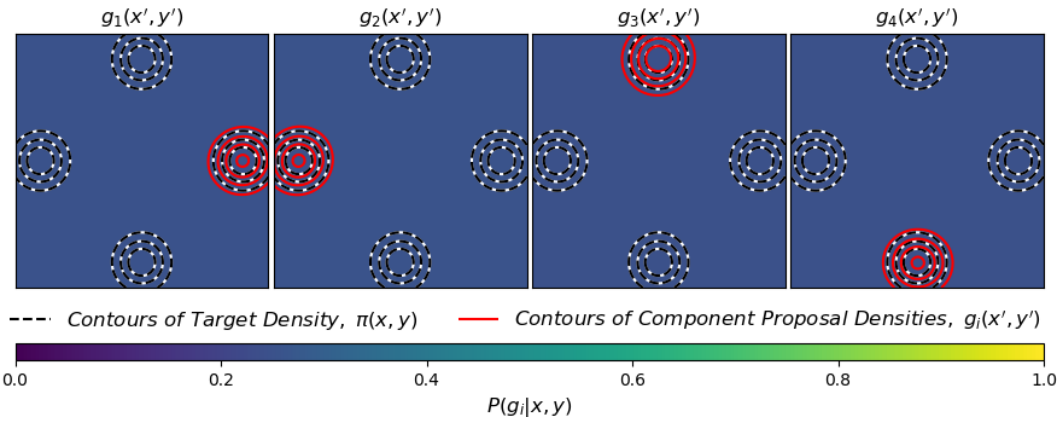
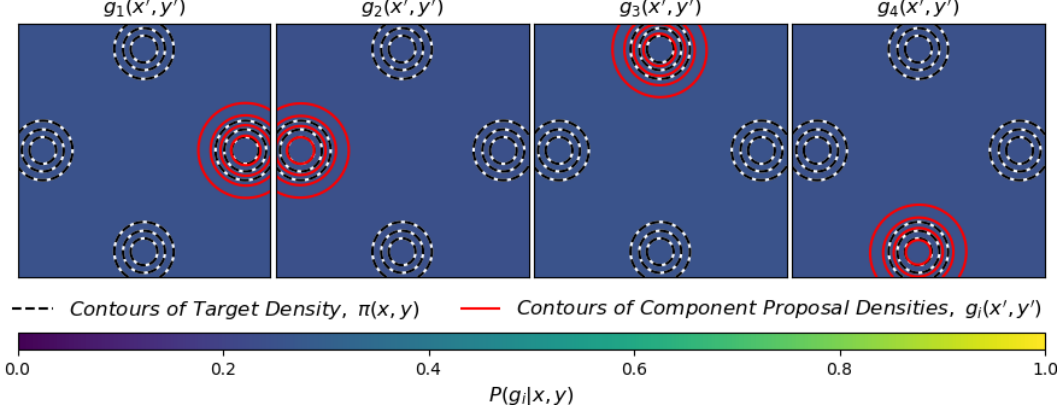


Figure 4: Comparison of position-dependent mixture proposals of Equation 3 obtained by optimizing GSM targeting an acceptance rate of 0.3. Each subplot illustrates the contours of a proposal component (in red) alongside a density plot of the probability of sampling from that component based on starting position.



F Further Details for Multi-Scheme Proposal Optimization

Our experiments with multi-scheme proposals utilize a distribution specified as follows:

$$\begin{aligned} \vec{n} &\sim \mathcal{N}\{\vec{0}; I\} \\ \vec{z}'|\vec{x}, \vec{n} &= \mu_{L,\theta}(T_\theta^{-1}(\vec{x})) + \Sigma_{L,\theta}(T_\theta^{-1}(\vec{x})) \odot \vec{n} \\ \vec{x}' &= \mu_{D,\theta}(\vec{x}) + \Sigma_{D,\theta}(\vec{x}) \odot T_\theta(\vec{z}') \end{aligned}$$

The target distribution is an equal mixture of 4 standard gaussians positioned in a cross formation with a maximal distance of 8 between component centers. The additive functions, $\mu_{L,\theta}$ and $\mu_{D,\theta}$, are specified by standard ReLU networks (input dimension 2, hidden dimension 16, 4 hidden layers, output dimension 2). The multiplicative functions, $\Sigma_{L,\theta}$ and $\Sigma_{D,\theta}$, are specified by standard ReLU networks (input dimension 2, hidden dimension 16, 4 hidden layers, output dimension 2) followed by component-wise exponentiation. The normalizing flow, T_θ , follows the NICE architecture [34], with additive coupling layers specified by standard ReLU networks (input dimension 1, hidden dimension 6, 3 hidden layers, output dimension 1). For this experiment, differing numbers of coupling layers are considered ($L = 8$ and $L = 3$). For optimization, 20000 gradient steps are taken, with each training batch taken from 8 starting points sampled i.i.d. from the target distribution from each of which 100 proposals are generated to calculate expected loss. Optimization is performed using the

Adam optimizer [36] with a stepsize of 3e-4. Optimized proposals that fall into local optima of the objective functions are discarded. For optimizing GSM [27], β is initially set to 0.5 and ρ_β is set to 0.02 and initialization is varied to ensure the target acceptance rate is attained. Acceptance rate, MSJD, and ESS are estimated for each optimized model based on 5 independent Markov Chains of 1000 proposals with starting points independently sampled from the target distribution. ESS relating to the second moments of the target distribution is estimated based on the Markov Chains obtained by component-wise squaring of the Markov Chains used to estimate the other performance measures. We utilize PyMC's [37] calculation of ESS, which considers both within-chain and between-chain variance. To gather statistics regarding the mean and standard error of reported variables, each optimization is replicated a total 5 times. Figures 7, 8, 9, and 10 show density plots of the multi-scheme proposals obtained following optimization using L2HMC's objective [13] and the GSM [27] with varying target acceptance rates. Figures 11, 12, 13, 14, 15, and 16 show density plots of the multi-scheme proposals obtained following optimization of all considered objective functions.

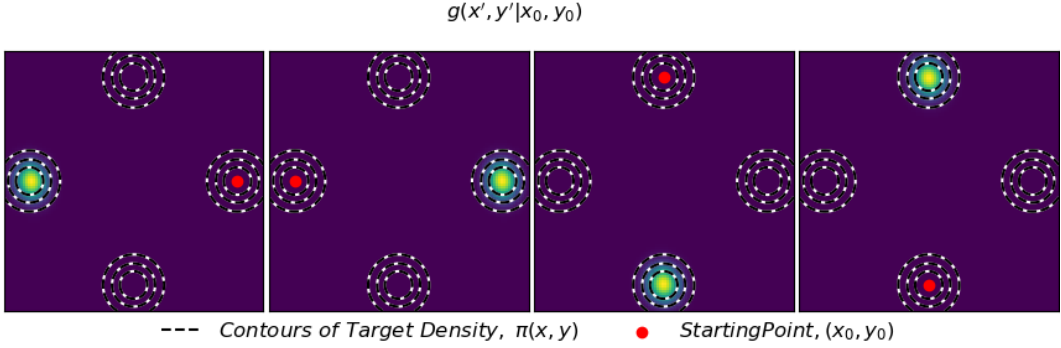


Figure 7: Comparison of multi-scheme mixture proposals (L=8) of Equation 4 obtained by optimizing L2HMC's objective. Each subplot illustrates the proposal distribution's density when sampling from a given starting position (in red).

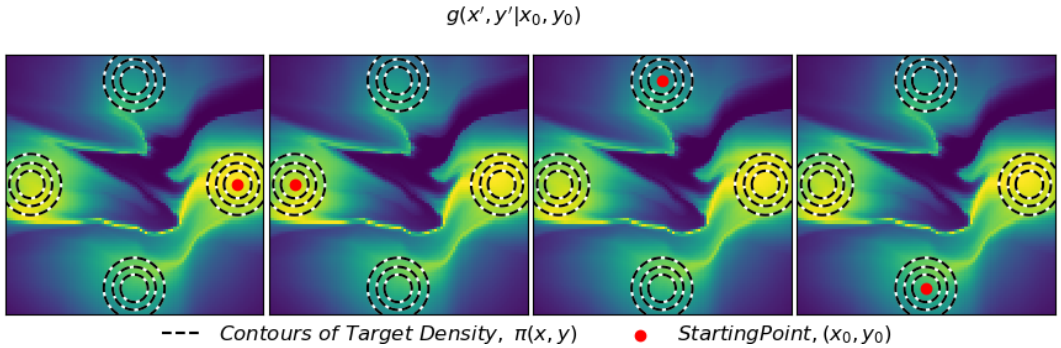


Figure 8: Comparison of multi-scheme mixture proposals (L=8) of Equation 4 obtained by optimizing GSM targeting an acceptance rate of 0.3. Each subplot illustrates the proposal distribution's density when sampling from a given starting position (in red).

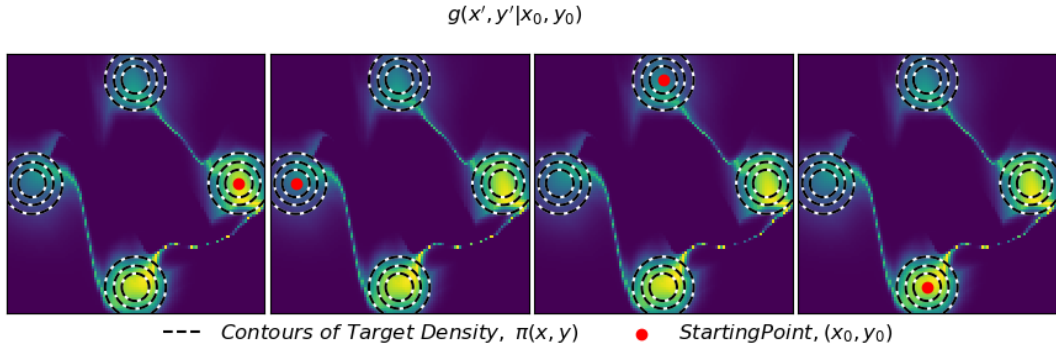


Figure 9: Comparison of multi-scheme mixture proposals (L=8) of Equation 4 obtained by optimizing GSM targeting an acceptance rate of 0.6. Each subplot illustrates the proposal distribution's density when sampling from a given starting position (in red).

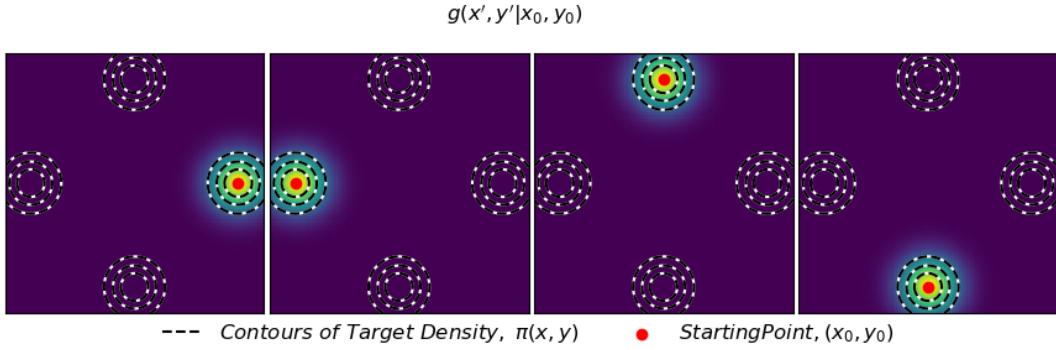


Figure 10: Comparison of multi-scheme mixture proposals (L=8) of Equation 4 obtained by optimizing GSM targeting an acceptance rate of 0.9. Each subplot illustrates the proposal distribution's density when sampling from a given starting position (in red).

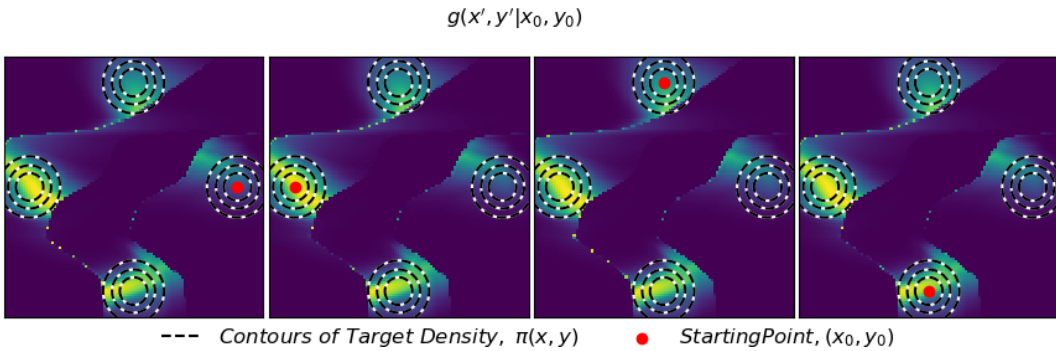


Figure 11: Comparison of multi-scheme mixture proposals (L=3) of Equation 4 obtained by optimizing our Ab Initio objective. Each subplot illustrates the proposal distribution's density when sampling from a given starting position (in red).

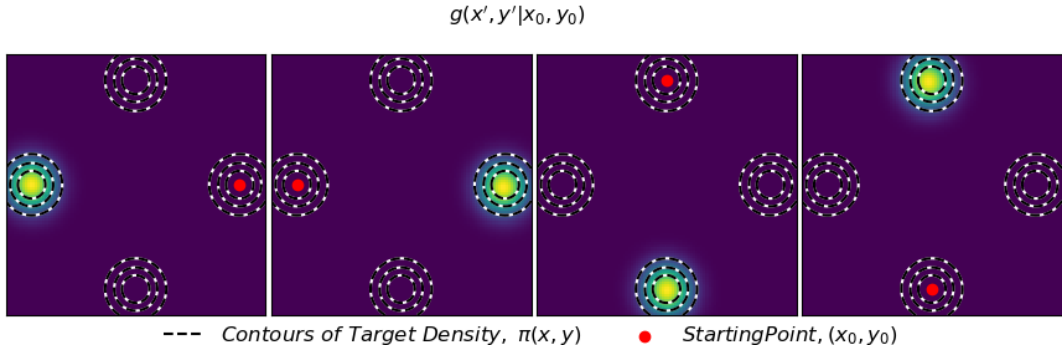


Figure 12: Comparison of multi-scheme mixture proposals (L=3) of Equation 4 obtained by maximizing MSJD. Each subplot illustrates the proposal distribution's density when sampling from a given starting position (in red).

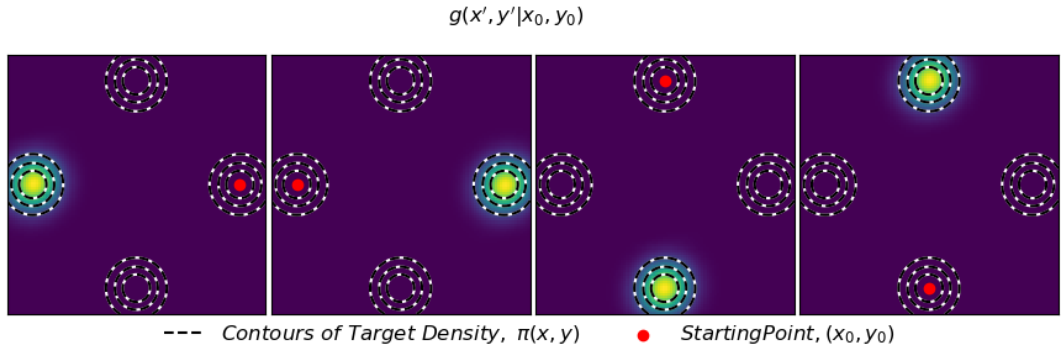


Figure 13: Comparison of multi-scheme mixture proposals (L=3) of Equation 4 obtained by optimizing L2HMC's objective. Each subplot illustrates the proposal distribution's density when sampling from a given starting position (in red).

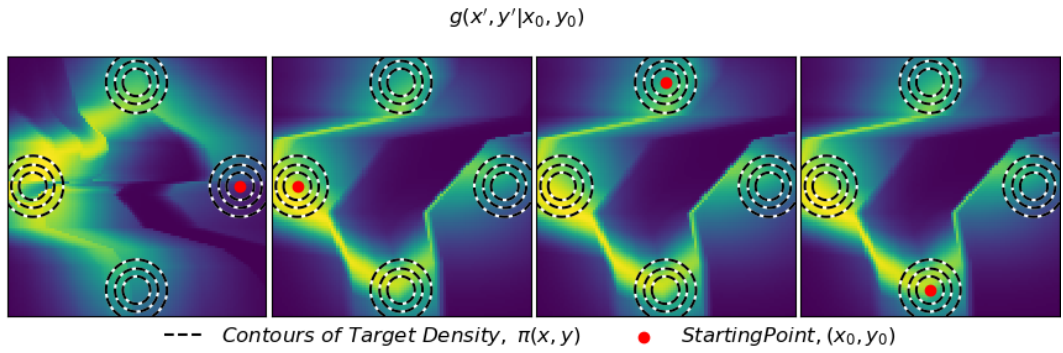


Figure 14: Comparison of multi-scheme mixture proposals (L=3) of Equation 4 obtained by optimizing GSM targeting an acceptance rate of 0.3. Each subplot illustrates the proposal distribution's density when sampling from a given starting position (in red).

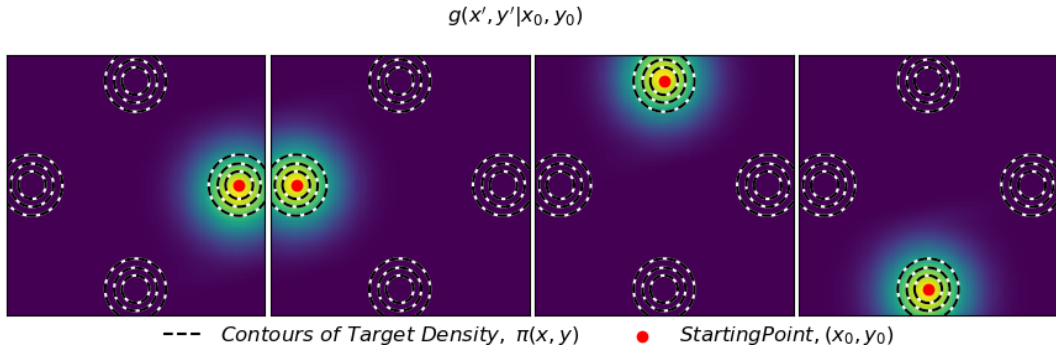


Figure 15: Comparison of multi-scheme mixture proposals (L=3) of Equation 4 obtained by optimizing GSM targeting an acceptance rate of 0.6. Each subplot illustrates the proposal distribution's density when sampling from a given starting position (in red).

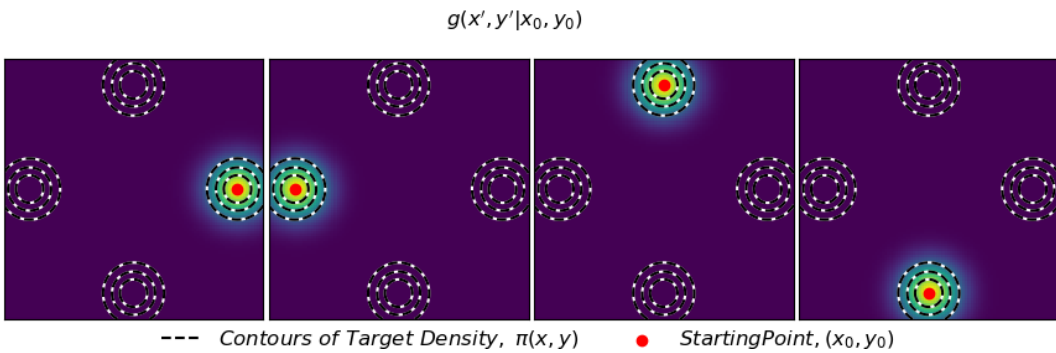


Figure 16: Comparison of multi-scheme mixture proposals (L=3) of Equation 4 obtained by optimizing GSM targeting an acceptance rate of 0.9. Each subplot illustrates the proposal distribution's density when sampling from a given starting position (in red).

G Further Details for Logistic Regression Posterior Sampling

For this experiment, we augment the target distribution with a number of auxiliary variables. Similar to the momenta in HMC, these augmenting variables are independent of the original data variables and are distributed following a standard multivariate gaussian. Proposal distributions are optimized to target the joint distribution of original and augmenting variables. For sampling, the augmenting variables are resampled before making each proposal, similar to the procedure employed in HMC. With one exception (the Ripley dataset) we found best results by using a number of augmenting variables, a , equal to twice the dimensionality of the original data, d .

This experiment again uses multi-scheme proposals, specified as follows:

$$\begin{aligned}\vec{n} &\sim \mathcal{N}\{\vec{0}; I\} \\ \vec{z}'|\vec{x}, \vec{n} &= \mu_{L,\theta}(T_\theta^{-1}(\vec{x})) + \Sigma_{L,\theta}(T_\theta^{-1}(\vec{x})) \odot \vec{n} \\ \vec{x}' &= \mu_{D,\theta}(\vec{x}) + \Sigma_{D,\theta}(\vec{x}) \odot T_\theta(\vec{z}')\end{aligned}$$

The target distribution is the posterior distribution of regression weights for logistic regression of various datasets from the UCI repository [35] and from Ripley [38]. The prior distributions used for regression weights are independent gaussians with a mean of 0 and a standard deviation of 10. The additive functions, $\mu_{L,\theta}$ and $\mu_{D,\theta}$, are specified by standard ReLU networks (input dimension $a+d$, hidden dimension (W) 3 ($a+d$), 4 hidden layers (D), output dimension $a+d$). The multiplicative functions, $\Sigma_{L,\theta}$ and $\Sigma_{D,\theta}$, are specified by standard ReLU networks (input dimension $a+d$, hidden dimension (W) 3 ($a+d$), 4 hidden layers (D), output dimension $a+d$) followed by component-wise exponentiation. The normalizing flow, T_θ , follows the NICE architecture [34], with additive coupling layers specified by standard ReLU networks (input dimension $\frac{a+d}{2}$, hidden dimension (W) 3 ($a+d$), 4 hidden layers (D), output dimension $\frac{a+d}{2}$). For this experiment, the same number of coupling layers is used ($L = 5$) for all datasets. Table 10 summarizes the network parameters used in this experiment.

Before each optimization, a long equilibrated Markov Chain is obtained following 500,000 proposals of HMC tuned to attain an acceptance rate of 0.65 (using hamiltorch's [39] implementation of HMC). A burn-in period of 1000 proposals is utilized for this HMC tuning and is discarded. For optimization, 40000 gradient steps are taken, with each training batch taken from 8 starting points sampled randomly from HMC Markov Chain and from each starting point 100 proposals are generated to calculate expected loss. Uniform sampling from this Markov Chain approximates i.i.d sampling from the target. Optimization is performed using the Adam optimizer [36] with a stepsize of 3e-4. For optimizing GSM [27], β is initially set to 0.5 and ρ_β is set to 0.02 and initialization is varied to ensure the target acceptance rate is attained. Acceptance rate, MSJD, and ESS are calculated solely based on original data dimensions and are estimated for each optimized model based on 5 independent Markov Chains of 20000 proposals with starting points independently sampled from the target distribution. ESS relating to the second moments of the target distribution is estimated based on the Markov Chains obtained by component-wise squaring of the Markov Chains used to estimate the other performance measures. We utilize PyMC's [37] calculation of ESS, which considers both within-chain and between-chain variance. To gather statistics regarding the mean and standard error of reported variables, each optimization is replicated a total 5 times. Tables 11, 12, 13, 14, and 15 summarize the sampling performance measures obtained following optimization, including minimum, median, and maximum one-dimensional ESS obtained across all dimensions of the original data variables. Minimum one-dimensional ESS is most indicative of sampling efficiency across the entire state space of the distribution and is therefore the focus of our comparisons.

Table 10: Specification of network parameters used in multi-scheme proposals for logistic regression sampling tasks.

	a	d	$\mu_{L,\theta}$ and $\mu_{D,\theta}$		$\Sigma_{L,\theta}$ and $\Sigma_{D,\theta}$		T_θ		
					W	D	W	D	L
			W	D	W	D	W	D	L
German Credit	21	21	126	4	126	4	126	4	5
Australian Credit	15	15	90	4	90	4	90	4	5
Heart	14	14	84	4	84	4	84	4	5
Pima	9	9	54	4	54	4	54	4	5
Ripley	6	3	27	4	27	4	27	4	5

Table 11: Results from optimizing multi-scheme proposal distributions targeting posterior distribution of logistic regression weights for German Credit dataset. Value means are reported to at most the first significant digit of standard error (reported in parentheses).

	Acc. Rate	MSJD	ESS per Proposal	
			x_i	x_i^2
Ab Initio	0.81(1)	0.30(1)	0.56(3)	0.49(7)
MSJD Opt.	0.77(2)	0.32(1)	0.52(7)	0.4(1)
L2HMC Obj.	0.76(2)	0.32(1)	0.54(4)	0.48(5)
GSM-90	0.90(1)	0.012(1)	0.005(1)	0.005(1)
GSM-60	0.61(3)	0.24(1)	0.40(3)	0.40(3)
GSM-30	0.29(5)	0.13(2)	0.13(4)	0.13(4)
HMC	0.65	0.201(3)	0.006(3)	0.005(3)
I.I.D. Resample	1.00	0.3700(3)	0.98(1)	0.983(3)

Table 12: Results from optimizing multi-scheme proposal distributions targeting posterior distribution of logistic regression weights for Australian Credit dataset. Value means are reported to at most the first significant digit of standard error (reported in parentheses).

	Acc. Rate	MSJD	ESS per Proposal	
			x_i	x_i^2
Ab Initio	0.85(1)	1.58(4)	0.63(4)	0.57(8)
MSJD Opt.	0.77(2)	2.39(3)	0.55(2)	0.53(3)
L2HMC Obj.	0.76(1)	2.39(3)	0.47(4)	0.41(7)
GSM-90	0.901(4)	0.088(3)	0.0105(2)	0.0105(2)
GSM-60	0.61(1)	1.23(2)	0.41(1)	0.42(1)
GSM-30	0.32(1)	0.71(3)	0.16(1)	0.16(1)
HMC	0.65	1.43(2)	0.02(1)	0.02(1)
I.I.D. Resample	1.00	1.901(4)	0.97(1)	0.97(1)

Table 13: Results from optimizing multi-scheme proposal distributions targeting posterior distribution of logistic regression weights for Heart dataset. Value means are reported to at most the first significant digit of standard error (reported in parentheses).

	Acc. Rate	MSJD	ESS per Proposal	
			x_i	x_i^2
Ab Initio	0.86(2)	1.03(4)	0.63(6)	0.58(7)
MSJD Opt.	0.81(1)	1.40(3)	0.69(3)	0.32(6)
L2HMC Obj.	0.82(1)	1.43(4)	0.73(4)	0.28(4)
GSM-90	0.900(3)	0.138(3)	0.034(2)	0.035(1)
GSM-60	0.59(2)	0.72(2)	0.34(3)	0.35(3)
GSM-30	0.29(3)	0.42(4)	0.13(2)	0.14(2)
HMC	0.65	0.70(1)	0.02(1)	0.02(1)
I.I.D. Resample	1.00	1.222(1)	0.97(1)	0.97(2)

Table 14: Results from optimizing multi-scheme proposal distributions targeting posterior distribution of logistic regression weights for Pima dataset. Value means are reported to at most the first significant digit of standard error (reported in parentheses).

	Acc. Rate	MSJD	ESS per Proposal	
			x_i	x_i^2
Ab Initio	0.88(3)	0.18(1)	0.7(1)	0.7(1)
MSJD Opt.	0.84(2)	0.28(1)	0.79(6)	0.13(6)
L2HMC Obj.	0.84(4)	0.27(1)	0.78(5)	0.14(8)
GSM-90	0.91(1)	0.186(3)	0.69(6)	0.68(6)
GSM-60	0.60(3)	0.14(1)	0.43(3)	0.44(3)
GSM-30	0.30(3)	0.08(1)	0.15(2)	0.15(2)
HMC	0.65	0.139(3)	0.007(2)	0.007(2)
I.I.D. Resample	1.00	0.2118(2)	0.98(1)	0.98(1)

Table 15: Results from optimizing multi-scheme proposal distributions targeting posterior distribution of logistic regression weights for Ripley dataset. Value means are reported to at most the first significant digit of standard error (reported in parentheses).

	Acc. Rate	MSJD	ESS per Proposal	
			x_i	x_i^2
Ab Initio	0.97(1)	0.48(1)	0.90(4)	0.88(4)
MSJD Opt.	0.92(1)	0.87(2)	1.35(6)	1.2(1)
L2HMC Obj.	0.91(2)	0.87(3)	1.4(1)	1.2(1)
GSM-90	0.90(1)	0.46(1)	0.82(3)	0.81(3)
GSM-60	0.61(2)	0.35(1)	0.50(1)	0.51(2)
GSM-30	0.30(1)	0.20(1)	0.20(1)	0.20(1)
HMC	0.65	0.202(5)	0.15(3)	0.18(3)
I.I.D. Resample	1.00	0.498(2)	1.00(1)	0.99(2)

The results for the Heart, Pima, and Ripley datasets exhibit the same behavior observed within the experiments involving the gaussian mixture target in Sections 7.1 and 7.2. Optimizing MSJD or L2HMC’s objective yields proposals whose behavior significantly deviates from i.i.d. resampling from the target distribution and result in a proposal MSJD much larger than what would be obtained following i.d.d. resampling from the target. As seen in Tables 13 and 14, the target distributions with the Heart and Pima datasets are similar to those with the gaussian mixture target in that this behavior is numerically evidenced by a severe decrease in ESS relating to estimation of the distribution’s second moments. From Table 15, we see that the target distribution with the Ripley dataset is such that this behavior is numerically evidenced by ESS calculations significantly greater than 1, which is indicative of the proposal distribution yielding greatly negative auto-correlations. Combined with the results from Section 7.1, these results demonstrate that this behavior is not the result of specific choices in proposal architecture or target distribution. We conclude that this sub-optimal behavior when maximizing MSJD or optimizing L2HMC’s objective occur when the proposal distribution allows sufficiently complex (relative to the target distribution) position dependence.

H Details Regarding Logistic Regression Datasets

All of the datasets used in the logistic regression sampling task are well established and are within the public domain (CC-PD Mark 1.0). Additional details regarding these datasets may be found in their respective collections [35, 38]. Although these datasets have a long history of use as benchmark tasks, we cannot entirely guarantee that their data was collected ethically. Additionally, even though these datasets do not appear to divulge personally identifiable data, we cannot guarantee that there is no way that these datasets could be used or combined with outside information to yield personally identifiable data. However, we do not believe that these datasets are particularly troublesome with regards to these concerns.